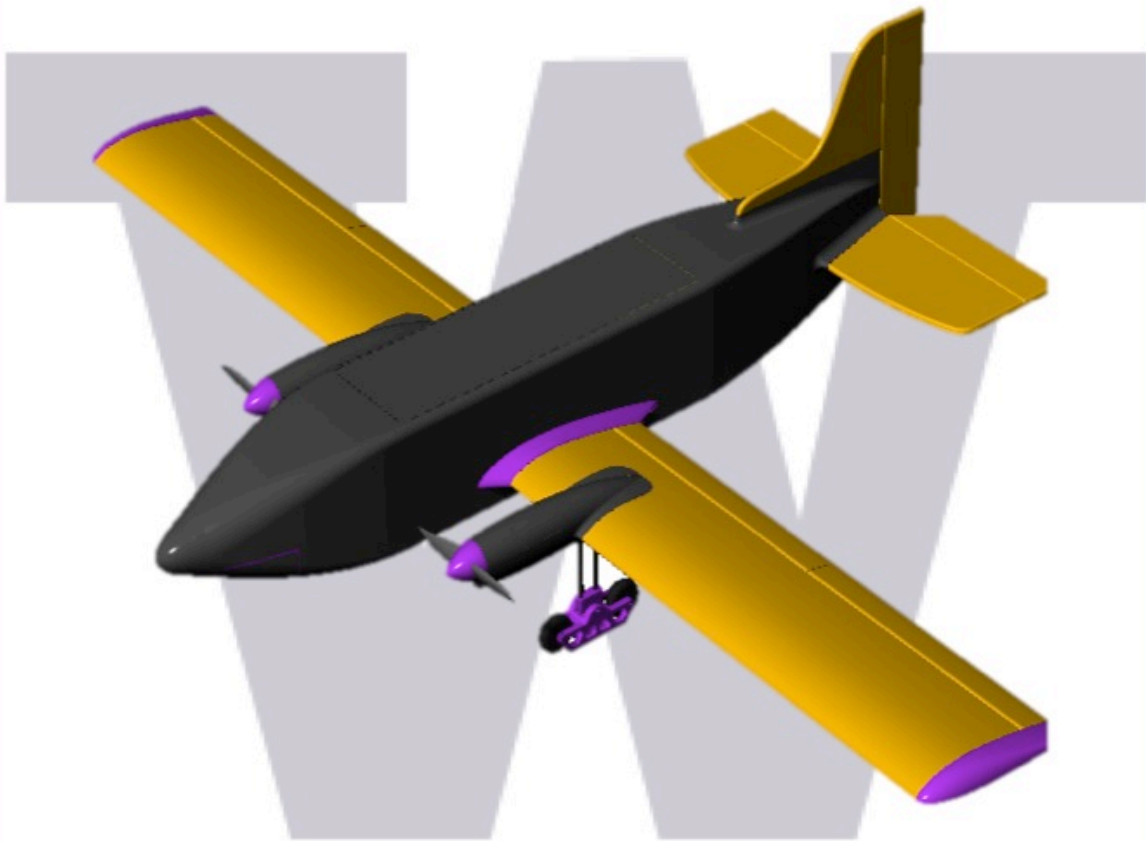




# **University of Washington Aircraft Design Report, 2013-2014 The Dawg Sled**



**Cessna/Raytheon/AIAA Design, Build, Fly Competition**

**2/24/2014**



## TABLE OF CONTENTS

<b>1. EXECUTIVE SUMMARY</b> .....	<b>4</b>
<b>2. MANAGEMENT SUMMARY</b> .....	<b>5</b>
2.1. DESIGN TEAM ORGANIZATION.....	<b>5</b>
2.2. PROJECT DESIGN SCHEDULE.....	<b>7</b>
<b>3. CONCEPTUAL DESIGN</b> .....	<b>8</b>
3.1 <i>MISSION SCORING AND REQUIREMENTS</i> .....	<b>8</b>
3.2 CONCEPTUAL DESIGN SELECTION.....	<b>12</b>
<b>4. PRELIMINARY DESIGN</b> .....	<b>15</b>
4.1 DESIGN ANALYSIS AND METHODOLOGY.....	<b>16</b>
4.2 DESIGN AND SIZING.....	<b>16</b>
4.3 ESTIMATES OF AIRCRAFT LIFT, DRAG, AND STABILITY CHARACTERISTICS.....	<b>19</b>
4.4 MISSION MODELS.....	<b>26</b>
<b>5. DETAILED DESIGN</b> .....	<b>27</b>
5.1 DIMENSIONAL PARAMETERS.....	<b>28</b>
5.2 STRUCTURAL CHARACTERISTICS.....	<b>28</b>
5.3 SYSTEMS AND SUBSYSTEMS DESIGN, COMPONENT SELECTION, INTEGRATION, AND ARCHITECTURE.....	<b>30</b>
5.4 WEIGHT AND BALANCE.....	<b>32</b>
5.5 DRAWING PACKAGE.....	<b>33</b>
<b>6. MANUFACTURING PLAN AND PROCESSES</b> .....	<b>39</b>
6.1 PRODUCTION PLAN AND SCHEDULE.....	<b>39</b>
6.2 MANUFACTURING PROCESS.....	<b>40</b>
<b>7. TESTING PLAN</b> .....	<b>42</b>
<b>8. PERFORMANCE RESULTS</b> .....	<b>45</b>
<b>9. References</b> .....	<b>46</b>



## NOMENCLATURE

$EW$	empty weight (lbs)
$N_{laps}$	number of laps completed
$N_{max\ l}$	maximum number of laps completed
$N_{cargo}$	number of cargo carried
$RAC$	rated aircraft cost
$SF$	size factor (ft)
$T$	time to complete Mission 3 (s)
$T_{min}$	minimum time to complete Mission 3 (s)



## 1. EXECUTIVE SUMMARY

This report details the design, manufacturing, and testing procedures used by the University of Washington DBF Team for the 2013-2014 Cessna Aircraft Company/Raytheon Missile Systems/AIAA Foundation Design/Build/Fly Competition. Engineering students from the University of Washington (UW) collaborated to complete an aircraft that would receive the highest score in the competition. The team is scored based on the product of its written report score and total mission score, divided by the rated aircraft cost, or the empty weight of the aircraft.

The theme for design of this year's aircraft was a "backcountry rough field bush plane." For the taxi mission, corrugated roofing had to be traversed, which is similar to the requirements for an actual bush plane, as they must be able to take off and land in sub-optimal ground and air conditions. In the preliminary design meetings it was determined that a tail-dragger, square-fuselage, low-wing aircraft was the optimal configuration for both the taxi and flight missions, due to the payload and performance requirements.

The "Dawg Sled" UW aircraft used a FX61-147 airfoil to provide enough lift to take off in the 40 feet of runway the team was limited to. The conventional empennage, with separate rudder and elevator, along with a streamlined, low-drag body allow for optimal aerodynamic performance while maintaining dynamic stability. Additionally, the team was limited to a 15 amp fuse, which led to the decision to use two motors, each with a single fuse connected to its own line of batteries.

It was determined that, in order to receive the highest possible score, all missions must be completed, while keeping the aircraft as light as possible. Much emphasis was placed on the taxi mission, as the total mission score is a product of the taxi score and flight score, and if the taxi mission is not completed, the total mission score will be reduced by 80%. It was for this reason that some aerodynamics of the aircraft were compromised to ensure it could navigate the corrugated roofing of the taxi mission. The main compromise was the use of landing skis in addition to wheels, which would enable the aircraft to move more smoothly over this obstacle.

The end system solution has the capability to traverse across the corrugated roofing panels while navigating around obstacles. The approximate take-off distance of the aircraft is 35 feet at a takeoff speed of 30 feet per second. Due to the high lift airfoil, and extensive wind tunnel testing, the aircraft is able to make short take offs in the prescribed field length. The maximum speed of the aircraft is estimated to be 60 mph, allowing the completion of 4 laps for Flight Mission 1. The aircraft is able to carry a maximum payload of 3.5 lb, which allows for a payload of 3 cargo blocks for Flight Mission Two, and successful completion of Flight Mission 3.



## 2. MANAGEMENT SUMMARY

The University of Washington Design, Build, Fly team is a small entity and all members collaborate on almost every aspect of the project. However, for purposes of organization and efficient management, five teams bear responsibility for the five main areas of project effort: aerodynamics, structures, manufacturing, stability and controls, and testing. Each team focuses on their specific area of work, and ensures that their group delivers project goals on time and within the allocated budget.

### 2.1 Design Team Organization

Figure 2.1 shows the organization of the UW DBF team.

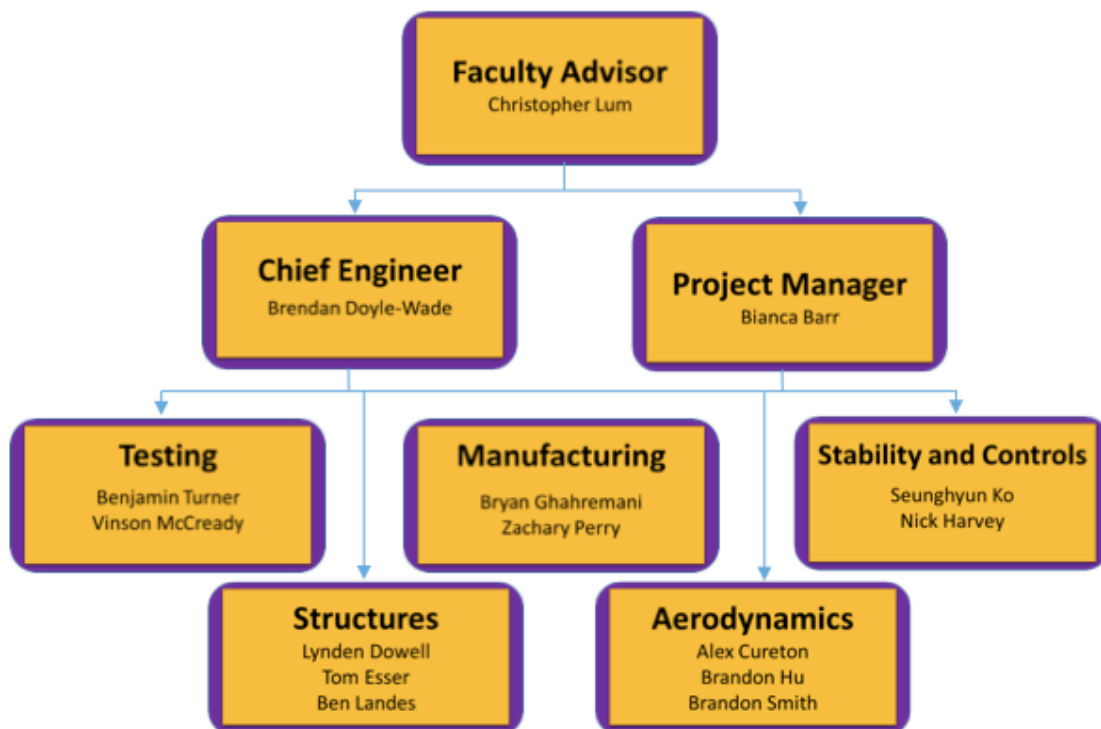


Figure 2.1. Team Organization Chart



### *2.1.1 Project Manager*

The team structure begins with the project manager overseeing team organization and major activities. The manager is primarily responsible for the coordination and communication among the group leads and team members. The project manager will use meetings and progress reports to facilitate team communication. Being the overseer of this project, a bulk of the report writing is also in the hands of the project manager.

### *2.1.2 Chief Engineer*

The chief engineer is responsible for the initial design and modeling of the aerodynamic and structural design of the aircraft. He is responsible for major decisions regarding the design and construction of the airplane. The chief engineer will act as the team pilot and coordinate all the groups to effectively and efficiently build all of the airplane models.

### *2.1.3 Testing*

The testing team will be responsible for all model tests, including the wind tunnel testing. The team will assist with the construction of test models and analyze data collected from various aircraft tests.

### *2.1.4 Manufacturing*

The manufacturing team must work very closely with design engineering. After receiving detailed designs or design modifications from the other teams, the construction team is responsible for the fabrication of the wind tunnel test model and subsequent aircraft. Facility use and safety training will need to be arranged by the lead of this team.

### *2.1.5 Stability and Controls*

The stability and controls team is responsible for the various aspects of the aircraft design, including stability, controls, navigation, and aircraft performance. This team must use data collected from testing to determine the most efficient and stable design. The team is responsible for the control surfaces and the bulk of the electronics on the aircraft.



### *2.1.6 Structures*

The structures team is responsible for choosing the best combination of materials and structural design that will result in a lightweight and efficient aircraft given the mission parameters. The structures team will also be responsible for designing the landing gear.

### *2.1.7 Aerodynamics*

The aerodynamics team is responsible for analyzing the aircraft's aerodynamic performance. This team will analyze the data and coordinate with all other teams to design the aircraft components so that they are aerodynamically efficient.

### *2.1.8 Faculty Advisor*

The faculty advisor will provide assistance, advice, and guidance to the entire team. The faculty advisor will also help coordinate meetings and provide the budget for

## **2.2 Project Design Schedule**

In order to effectively schedule the designing, manufacturing, and testing of all aircraft models, a milestone chart was created. The chart shows all major phases of the project. Both the projected time periods and actual time periods are shown for each phase. The project began at the beginning of the 2013-2014 University of Washington school year on September 25 2013 and continued until the competition on April 11-13 2014. The planned schedule is designed with more time than truly needed in order to account for unforeseen problems that could potentially slow down the project. The milestone chart is shown in Figure 2.2:

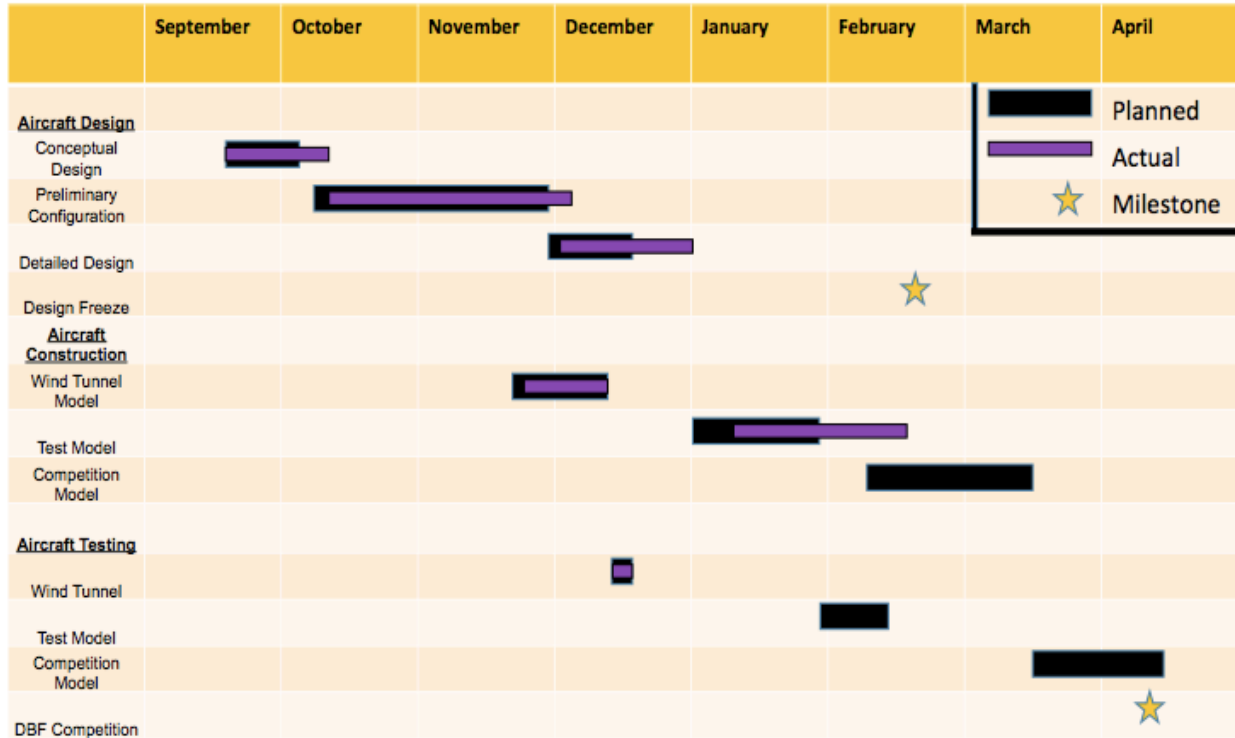


Figure 2.2. Project design schedule.

### 3. CONCEPTUAL DESIGN

In the conceptual design phase of the project, the UW DBF team took the 2014 mission and scoring requirements as well as experience from past years into consideration while conducting a preliminary trade study. This trade study allowed for the research of various aircraft configurations and how they would affect the different mission parameters in order to maximize the possible score for this year's competition.

#### 3.1 Mission scoring and Requirements

The 2014 AIAA DBF competition is comprised of a Ground Taxi Mission and three Flight Missions. Each of the flight mission scores is added together and then multiplied by the pass/fail score from the ground mission. The goal is to attain the highest possible score which is achieved by completing all four missions, abiding by the competition constraints, as well as optimizing important aircraft design parameters such as speed, weight, size, and payload capacity.



### 3.1.1 General Requirements

Each mission to be completed has a general set of requirements to be upheld during the competition. The aircraft must not drop any structure/components during flight, and must take-off completely under its own power. The propeller must be powered by an unmodified over-the-counter electric motor and the propeller(s) must be commercially produced as well. Standard NiCad or NiMH batteries are to be used and must be limited in current draw by a 15 amp fuse. The battery pack(s) maximum weight limit is 1.5 lbs. The aircraft must have a ground clearance measured by passing a 2x4 under each wing during inspection.

### 3.1.2 Ground Taxi Mission

The ground taxi mission must be attempted before Flight Mission 2. This mission simulates the conditions for taxiing across a rough field. The mission will take place on a 40' x 8' Palruf Roofing Panel. This panel is has corrugation aligned normal to the long axis of the course with spacing of 3" wide x 0.625" high. At 1/3 and 2/3 the course length there will be to obstacles extending from the centerline of the course to one edge. The layout for the Taxi Mission course can be seen below in Fig. 3.1.

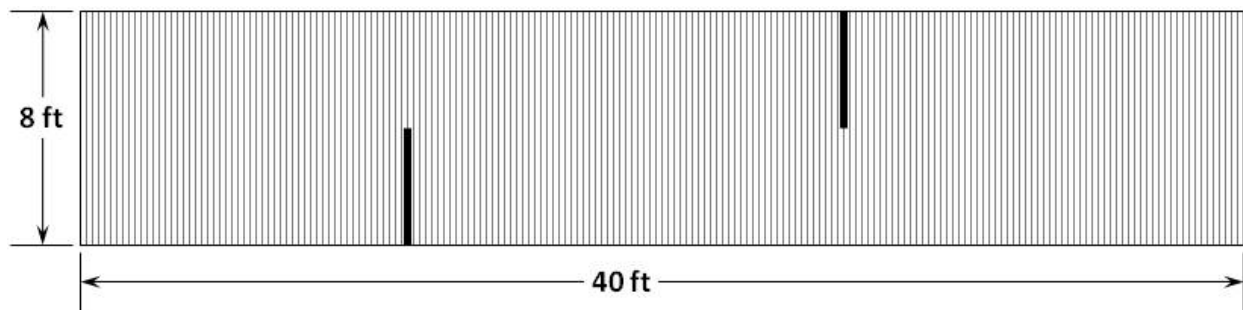


**Fig. 3.1:** Taxi Mission Course Layout

### 3.1.3 Mission 1 – Ferry Flight

The goal of the first mission is to complete as many laps as possible around the flight course within a four minute flight time. The timer starts when the throttle is advanced for the (first) take-off. A lap is complete when the aircraft crosses over the start/finish line in the air. The plane must take off within the prescribed field length and a successful landing must be completed in order for the team to receive a score. During this flight no payload will be installed. The score for mission one is normalized by the performance of the best team and can be computed with the following formula:

$$M1 = 2 * \frac{N_{Laps\ Flown}}{N_{Max\ Laps\ Flown}}$$



Where,  $N_{\text{Laps Flown}}$  represents the number of laps completed by the current team, and  $N_{\text{Max Laps Flown}}$  represents the maximum number of laps completed during the competition.

### 3.1.4 Mission 2 – Maximum Load Mission

The goal of the second mission is to complete three laps while carrying a maximum load of cargo. The cargo is represented by 6"x6"x6" wooden blocks, ballasted to 1 lb each. All of the cargo is to be carried internally and must be properly secured. The aircraft must take-off within the prescribed field length and a successful landing must be completed in order for the team to receive a score. The score for mission two is normalized by the maximum number of cargo flown by the best team and can be computed with the following formula:

$$M2 = 4 * \frac{N_{\text{Cargo Flown}}}{N_{\text{Max Cargo Flown}}}$$

where,  $N_{\text{Cargo Flown}}$  represents the number of 1 lb blocks carried by the current team, and  $N_{\text{Max Cargo Flown}}$  represents the maximum number of 1 lb blocks carried during the competition.

### 3.1.5 Mission 3 – Emergency Medical Mission

The goal of the third mission is to complete a three-lap flight while carrying a two sets of medical passengers. Each set is comprised of two components: a patient and an attendant. The patient is simulated by a wooden block 9" long x 4" wide by 2" high oriented flat and lengthwise. Each patient will weigh 0.5 pounds. The attendant is positioned beside the patient and is simulated by a wooden block 6" tall x 2" wide x 4" long. Each attendant will weigh 0.5 pounds. The patient/attendant configuration can be seen below in Fig. 3.2.

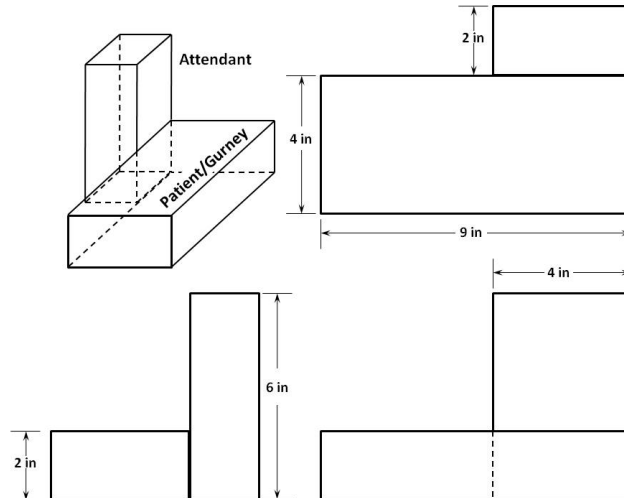


**Fig 3.2:** Patient/attendant payload configuration for Mission 3

There are several constraints defining the configuration of the patient/attendant sets inside the aircraft:

- The attendant must be oriented vertically and the patient must be horizontal and flat
- The attendant must be immediately adjacent to the patient
- The patients must be separated by a minimum of 2” on each side or above/below
- At least 2” above the patient must be “air space” comprising of no structure or aircraft systems
- The attendants must be separated by at least 2”

The aircraft must take-off within the prescribed field length and a successful landing must be completed in order for the team to receive a score. The timer starts when the throttle is advanced for the (first) take-off and ends when the airplane passes over the finish line (in the air) upon the completion of the last lap. The score for mission three is normalized by the time flown by the fastest team and can be computed with the following formula:

$$M3 = 6 * \frac{\text{Fastest Time Flown}}{\text{Time Flown}}$$

Where, Fasted Time Flown represents the flight time of the fastest team and Time Flown represents the flight time of the current team.

### 3.1.6 Scoring Summary

The team’s total score will be determined by the following formula:



$$Total\ Score = \frac{Written\ Report\ Score * [TS * (M1 + M2 + M3)]}{Rated\ Aircraft\ Cost}$$

where Rated Aircraft Cost is a function of the aircraft's empty weight (EW) which can be found by the following formula:

$$EW = Max(EW1, EW2, EW3)$$

### 3.2 Conceptual Design Selection

The optimum configuration for the aircraft was determined by completing a conceptual design trade study. This trade study helped determine the best configuration for seven of the main aircraft components which were the: landing gear, propeller, number of motors, body configuration, wing configuration, fuselage, and stabilizer configuration. A set of design criteria was formulated using the mission requirements and for each component a set of possible configurations was considered and given a score aligning with these criteria. These point values were summed and the configuration with the highest overall score was chosen for each aircraft component. The conceptual design trade study can be seen below in Fig. 3.3. The rows highlighted in purple indicate the component of the aircraft, while the rows highlighted in yellow indicate the configuration that had the greatest total in its category.



	Mission Requirements									
	Ground Taxi Mission			All Flight Missions		Flight Mission 1		Flight Mission 2		Totals
Landing Gear	RAC	Navigate around obstacles	Same payload as FM3	Take off within 40 feet	Land successfully	Max # of Laps within 4 mins	No payload	3 Lap internal cargo flight	Maximum number of cargo	
Tricycle	1	2	0	1	2	1	0	0	0	7
Tail Dragger	2	1	0	2	1	2	0	0	0	8
<b>Propeller</b>										
Pusher	0	1	0	1	1	1	1	2	0	7
Puller	0	2	0	2	2	1	1	1	0	9
<b>Number of Motors</b>										
1 motor	0	1	0	1	1	1	1	0	1	5
2 motors	0	2	0	2	2	1	1	0	2	10
<b>Configuration</b>										
Conventional	3	4	0	4	4	2	0	3	0	20
Canard	2	3	0	3	1	4	0	2	0	15
Flying Wing	4	2	0	1	2	3	0	1	0	13
Monoplane	2	2	0	2	2	2	0	2	0	12
Biplane	1	1	0	1	1	1	0	1	0	6
Tandem Wing	1	1	0	2	3	1	0	4	0	12
<b>Wing Placement</b>										
High wing	1	1	0	1	3	1	0	2	0	9
Mid Wing	1	2	0	2	2	2	0	1	0	10
Low wing	1	3	0	3	1	3	0	2	0	13
<b>Fuselage</b>										
Lifting Body	1	1	2	1	1	2	1	1	1	11
Conventional	1	1	1	1	2	1	2	2	2	13
<b>Stabilizers</b>										
Conventional	3	4	4	4	4	3	0	0	0	21
T-tail	2	4	3	3	5	3	0	0	0	20
H-tail	1	3	4	4	2	3	0	0	0	19
V-tail	5	2	2	2	2	2	0	0	0	15
A-tail	4	1	1	1	1	1	0	0	0	9

Fig. 3.3. Aircraft Component Trade Study



### *3.2.1 Body Configuration*

The body configuration took into account two different body styles: lifting body, and conventional. The lifting body was determined to be good for carrying high loads during flight. This configuration also provides a very efficient use of body volume. The drawback to this option is the limited flight speed due to large fuselage sections and their increased drag. The second option is a conventional fuselage. This fuselage was chosen due to its ability to fly faster while still carrying a fair amount of cargo.

### *3.2.2 Wing Configuration*

The wing configurations to choose from included: conventional, canard, flying wing, monoplane, biplane, and tandem wing. The conventional configuration has a high stability and overall good maneuverability. The canard configuration provides good stall characteristics, although it also exhibits reduced pitch stability and yaw maneuverability. The flying wing configuration has a good speed range and in ideal situations can be more efficient than conventional setups. The drawback to using the flying wing configuration is its reduced carrying capacity as well as difficult flight control ability. The monoplane configuration is more efficient than the biplane configuration and is also easy to construct, while the biplane is good for high lift/slow flight situations. Lastly, the tandem wing configuration which has the possibility of being highly efficient depending on wing placement, although it lacks maneuverability. The conventional wing was chosen due to its ability to maneuver around obstacles and also its ability to be controlled more easily for take-off and landing.

### *3.2.3 Wing Placement*

Three configurations were considered for wing placement: high wing, mid wing, and low wing. A high wing would provide more stability than a low wing but lacks in stability compared to the other options. A low wing would be less stable during flight but allow for more maneuverability. The low wing would also allow for better utilization of ground effects on take-off and landing. The mid wing would be a compromise between high and low wing placement. The low wing was chosen due to its maneuverability characteristics which will lend to success in many mission requirements.

### *3.2.4 Stabilizer Configuration*

Five different configurations for stabilizer were considered: conventional, T-tail, H-tail, V-tail, and A-tail. The conventional stabilizer configuration is beneficial due to its simple construction as well as good stability characteristics. The T-tail configuration is more complex in construction due to the necessary



reinforcement of the horizontal stabilizer although it may allow for more maneuverability. The H-tail configuration takes up less vertical space and allows for a more efficient horizontal stabilizer. However, the H-tail is also harder to construct due to more complex structures and is also often heavier. The V-tail configuration is more efficient in theory due to lower surface area. The V-tail is also beneficial due to simpler construction, however, some adverse flight characteristics may arise due to this configuration. The A-tail configuration exhibits improved stall characteristics but may cause issues with ground clearance. The conventional configuration was chosen due to its simple construction and enhanced stability characteristics.

### *3.2.5 Propeller*

The propeller choices consisted of a pusher propeller versus a puller propeller. The puller propeller was chosen because it allowed for easier takeoff as well as a faster flight time.

### *3.2.6 Number of Motors*

The options for number of motors were limited to either 1 or 2 motors. 2 motors were chosen because they allowed for easier takeoff as well as a faster flight time and maximum carrying capacity.

### *3.2.7 Landing Gear*

Two landing gear configurations were considered during the trade study: tricycle and tail dragger landing gears. The tricycle landing gear provides good ground stability, however, they are heavier than tail draggers. Tail draggers allow for high ground maneuverability and are lighter than tricycle landing gears. The tail dragger landing gear configuration was chosen because it allowed for reduced aircraft weight as well as improved ground maneuverability, which will prove helpful in the ground taxi mission.

## **4. PRELIMINARY DESIGN**

In the preliminary design phase, our team used the results from conceptual design to determine sizing and performance parameters for the aircraft's relevant systems. The attributes of many different features and their impact on the total system performance were closely analyzed. This section will explain the reasons for configuration sizing choices, and demonstrate the decision process utilized in establishing the configuration that led to the maximum performance.



## 4.1 Design Analyses and Methodology

Since the various systems and subsystems of an aircraft are dependent on one another, our team relied on an iterative design process in order to develop an aircraft that would obtain the highest possible score at competition. The design wheel shown in Fig. 4.1 illustrates the methodology utilized by our team.

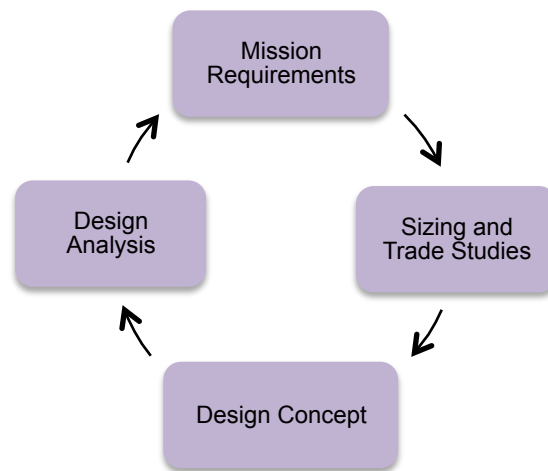


**Fig. 4.1.** Design wheel process for the preliminary design

The preliminary design process began with the mission requirements. The mission requirements were incorporated into the sizing and trade studies. Next, the sizing was implemented into the design concept. After a concept was created, the design was analyzed and compared with the mission requirements.

The process began with a close examination of the various degrees of freedom of the airplane design within the chosen configuration constraints. Fuselage size, propulsive power, wing size, tail size, payload weight, and overall weight were evaluated from a design perspective. The assumptions made were validated in the wind tunnel, and the airplane design was tuned based on the results of the wind tunnel test.

## 4.2 Design and Sizing

Design and sizing trades were utilized in the development of aircraft systems in order to investigate the effect of certain systems on the vehicle's overall flight score. These trade studies began with initial estimates for sizing and performance parameters, and were updated successively as the design progressed.



#### 4.2.1 Variation of score with number of cargo carried

In order to relate the total weight of the aircraft to the weight of the payload, a payload ratio,  $\lambda$ , was defined:

$$\lambda = \frac{\text{payload weight}}{\text{empty weight} + \text{payload weight}}$$

The plane was designed with the goal of a payload ratio of  $\lambda = 0.6$ . The flight score was related to the number of cargo by relating the velocity and weight as a function of the payload ratio. The velocity was related to the weight by holding the power available constant, and varying the number of cargo. Figure 4.2 shows a plot of the total flight score vs. number of cargo carried:

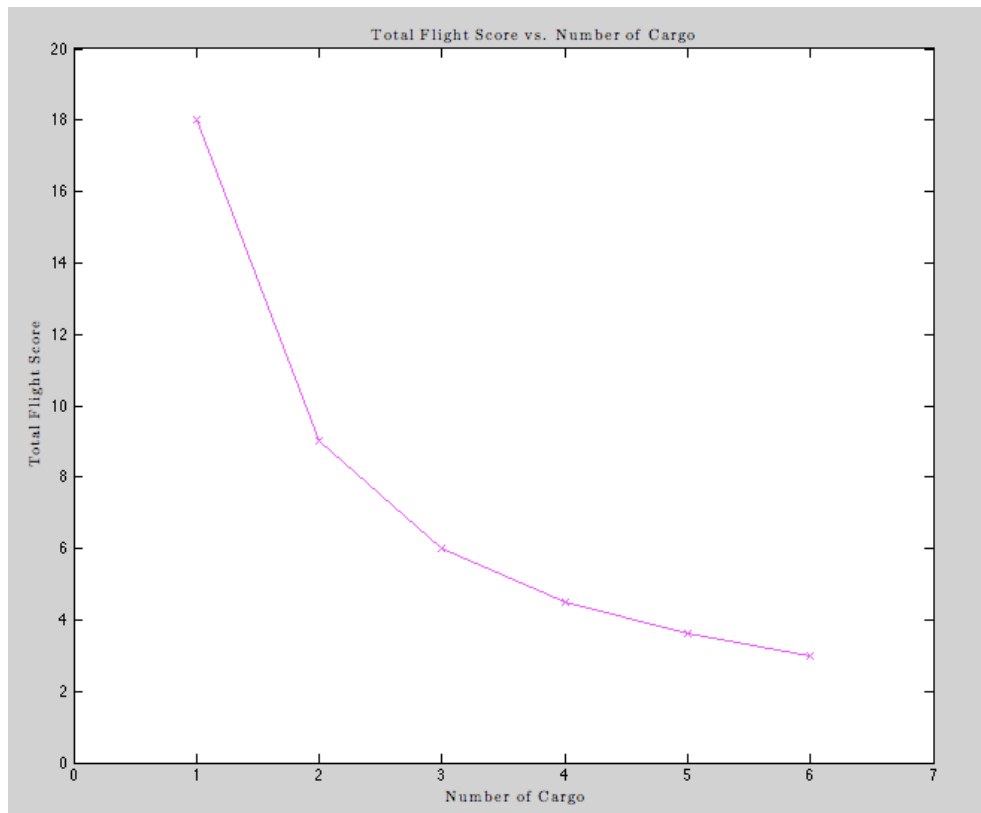


**Fig. 4.2. Effect of number of cargo on total flight score.**

It can be seen that a plane designed to hold only one cargo will yield the highest flight score. However, the dimensions of three cargo placed end to end is 18" x 6", while the constraints of the emergency medical mission requires the same dimensions of 18" x 6". Since the plane must be designed with the



dimension constraint of 18" x 6" for the emergency medical mission, it is decided that the plane will carry three cargos in order to increase the score of flight mission two.

#### 4.2.2 Wing Sizing

The minimum takeoff distance imposes a significant limitation on the aircraft design. Because power output is limited, the takeoff distance is directly proportional to the weight and wing area of the aircraft. The heavier the load, the bigger the wing must be to achieve liftoff within 40 feet. The overall takeoff weight became the first evaluative obstacle. Assumptions had to be made about the weight of craft and the weight of the payload, even though no detailed design had been done. These estimates were based on a takeoff velocity calculated using an iterative method in MATLAB. This calculation accounted for changing lift, drag, and power during the take off roll. Difficulty was encountered in calculating an accurate available power curve because of unknown motor performance and propeller efficiency. Because these assumptions would motivate the entire design, it was decided that a power test should be performed. This was conducted in the University of Washington 3' x 3' Low Speed Wind Tunnel. A motor and prop were chosen based on previous experience, and were mounted on a six-component force transducer, as shown below. The power came from a DC power supply, and an optical tachometer was used to measure RPM so that prop efficiency could be determined. The tunnel was run at an array of wind speeds designed to envelop the predicted flight regime, and thrust and power output were measured at each speed. Figure XX shows the motor and propeller mounted in the 3' x 3' Low Speed Wind Tunnel.

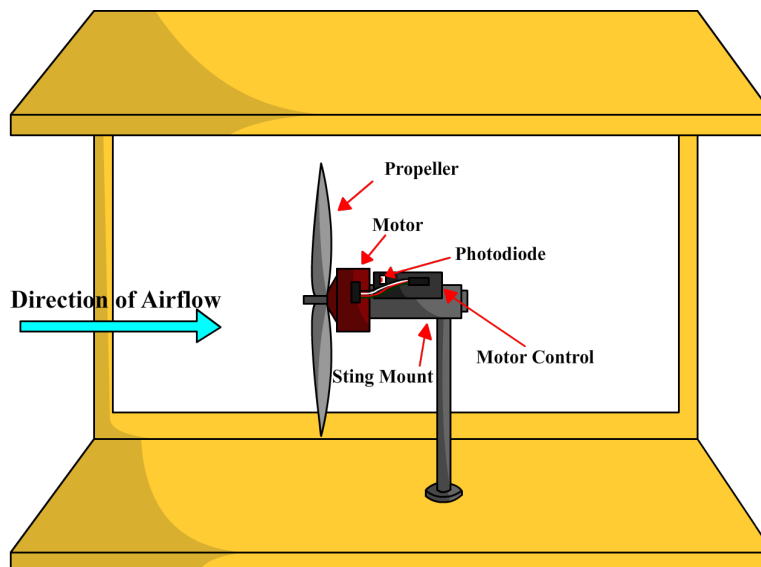


**Fig. 4.3.** Power testing of propeller and motor to determine power available for take-off roll.

Based on the results of the power test, it was found that a top speed of 32 ft/s could be reached within the takeoff box. After computing the takeoff velocity, a variety of airfoils were examined to see which ones



would provide optimal performance and necessary lift for the smallest total wing area. It was found that for an assumed mass payload fraction of 60%, the FX61-147 airfoil would be ideal for producing the lift needed in cruise. The wing in cruise configuration was designed to have an aspect ratio of 7, a total area of 553 in<sup>2</sup>, a wing span of 70.5 in, and a chord of 7.84 in.

#### 4.2.3 Tail Sizing

For initial tail sizing, the stability of the aircraft had to be considered. As a conventional tail design was chosen, the areas to consider for all stability calculations corresponded to the vertical and horizontal areas. The tail volume coefficient method was used to find the tail's horizontal area [1]:

$$S_{HT} = \frac{c_{HT} * \text{wing span} * \text{wing area}}{L_T}$$

The horizontal tail volume coefficient,  $c_{HT}$ , was estimated to be 0.5 for an RC aircraft with higher wing loading.  $S_{HT}$  represents the horizontal tail surface area.  $L_T$  is estimated as the distance between the wing and tail quarter chords.  $L_{HT}$  was picked to be approximately 22 in and  $S_{HT}$  was calculated to be 117 in<sup>2</sup>.

The tail volume coefficient method was also used to find the tail's vertical area[1]:

$$S_{VT} = \frac{c_{VT} * \text{wing span} * \text{wing area}}{L_T}$$

The vertical tail volume coefficient,  $c_{VT}$ , was estimated to be 0.03 for an RC aircraft with higher wing loading.  $S_{VT}$  represents the vertical tail surface area; it was calculated to be 46.9 in<sup>2</sup>.

### 4.3 Estimates of Aircraft Lift, Drag, and Stability Characteristics

After the establishment of initial aircraft dimensions, a wind tunnel test was needed to verify the aerodynamic performance of the design. A model was constructed out of insulation foam and copper tube spars, and mounted in the Kirsten Wind Tunnel at the University of Washington Aeronautical Laboratory. The purposes of the test were to explore the performance characteristics of the wing and establish the geometry of the flight surfaces relative to the fuselage. Because wing performance was not yet known, the test was conducted without tail surfaces. Following the test, a tail was designed to provide the control authority that the data indicated was needed. The optimum angle of incidence of the wing was determined. The behavior of the airplane at many different attitudes was tested, and the stability characteristics were experimentally verified. The proximity of the Kirsten Wind Tunnel and ease of testing



offered an excellent alternative to exhaustive computer simulation, and provided very accurate and reliable design information. Figures 4.4 and 4.5 show the wind tunnel model installed on the mounting strut in the Kirsten Wind Tunnel.

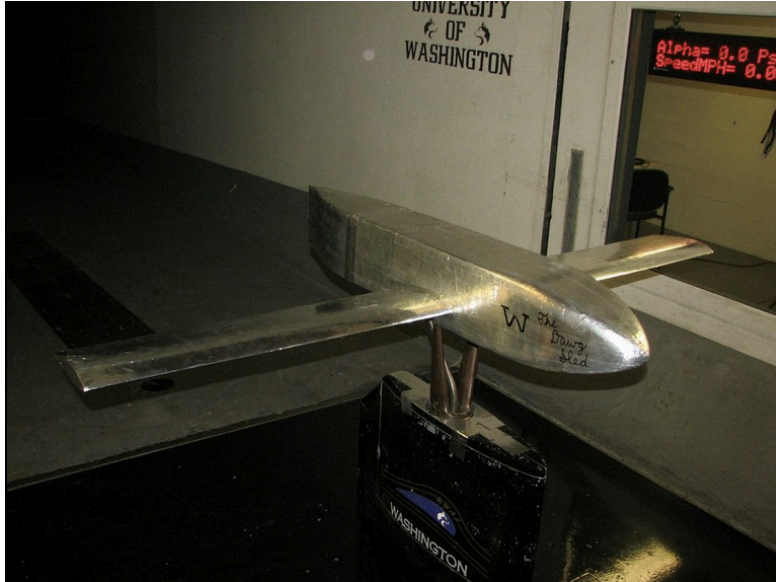


**Fig. 4.4.** A front view of the model mounted in the Kirsten Wind Tunnel.



**Fig. 4.5.** A rear view of the model mounted in the Kirsten Wind Tunnel.



The model was tested at dynamic pressures of  $q = 1$  psf and  $q = 6$  psf. The dynamic pressure of  $q = 1$  psf simulated take-off conditions, while the dynamic pressure of  $q = 6$  psf simulated conditions at maximum cruising speed. The model was tested at pitching angles from  $-10^\circ$  to  $+18^\circ$ . The DBF competition this year is taking place in Wichita, Kansas which historically has windy conditions for aircraft. In order to determine the characteristics of the aircraft in crosswind conditions, yaw angles were tested from  $-12^\circ$  to  $+12^\circ$ . Figure XX shows the coefficient of lift vs. angle of attack for the aircraft at  $q = 1$  psf while Fig. 4.6 shows the coefficient of lift vs. angle of attack at  $q = 6$  psf.

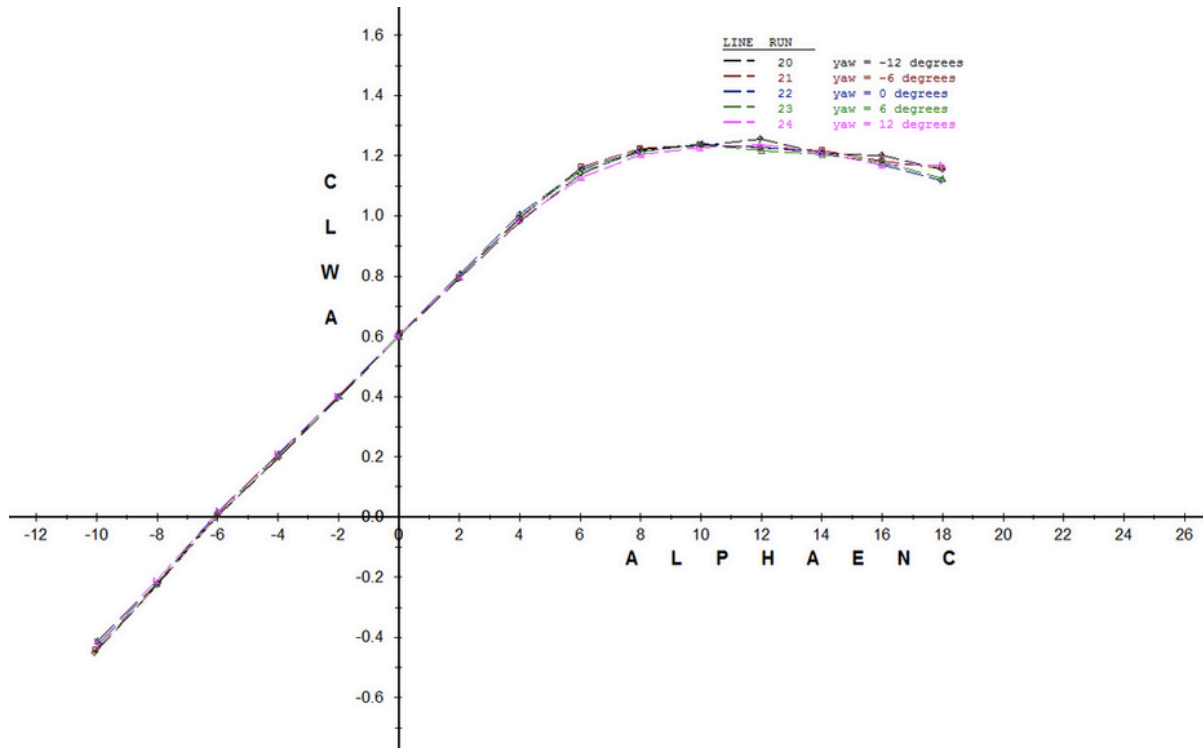


Fig. 4.6. Coefficient of lift vs. angle of attack at  $q = 1$  psf.

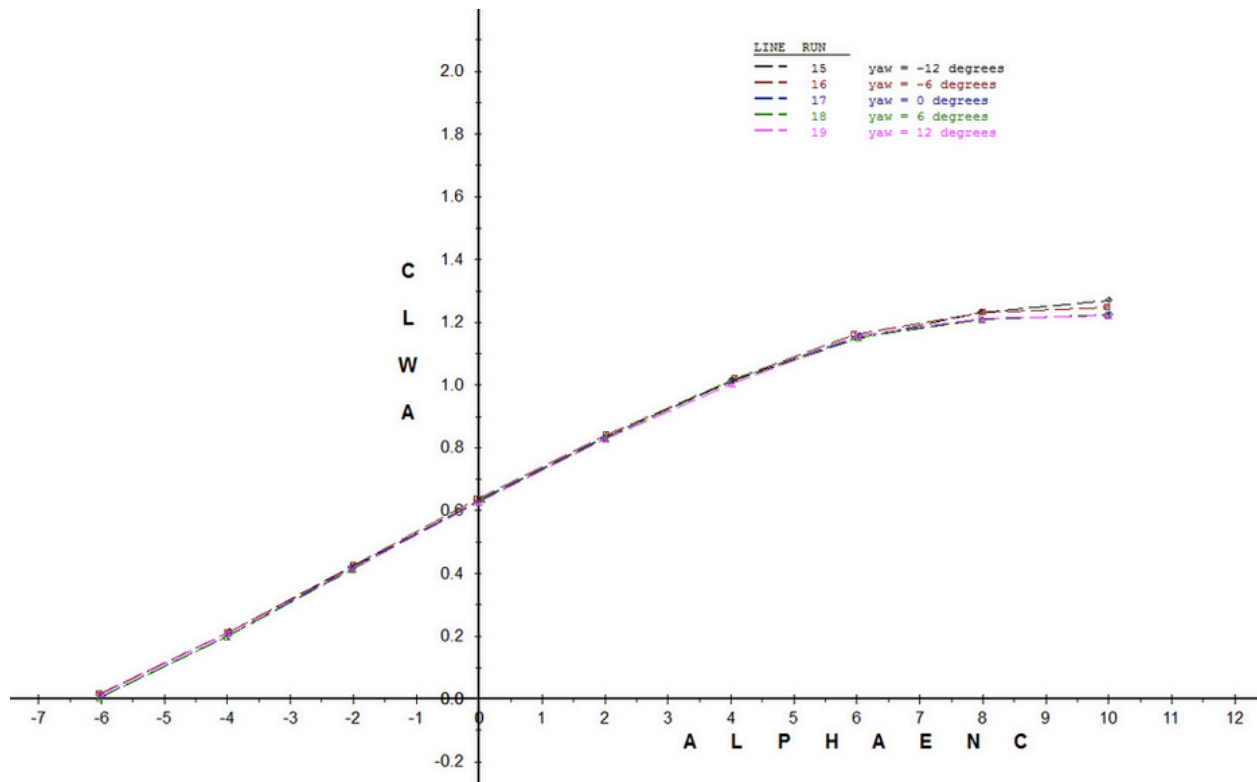


Fig. 4.7. Coefficient of lift vs. angle of attack at  $q = 6$  psf.

The maximum lift that the wing produces at  $q = 1$  psf is  $c_{l,max} = 1.25$  which can be seen in Fig.4.6. It was calculated that this value of  $c_{l,max}$  is sufficient for the aircraft to take off within the prescribed field length of 40 ft. The lift characteristics shown in Fig. 4.7 at maximum cruise speed conditions are desirable. The airfoil produces sufficient lift in order to maintain steady and level flight at a range of angles of attack. The stall characteristics of the wing at both dynamic pressures are also desirable. The wing stalls at  $\alpha = 12^\circ$  for takeoff conditions and at  $\alpha = 10^\circ$  at maximum cruise velocity.

The coefficient of drag vs. angle of attack is shown in Fig. 4.8 and 4.9 for each dynamic pressure.

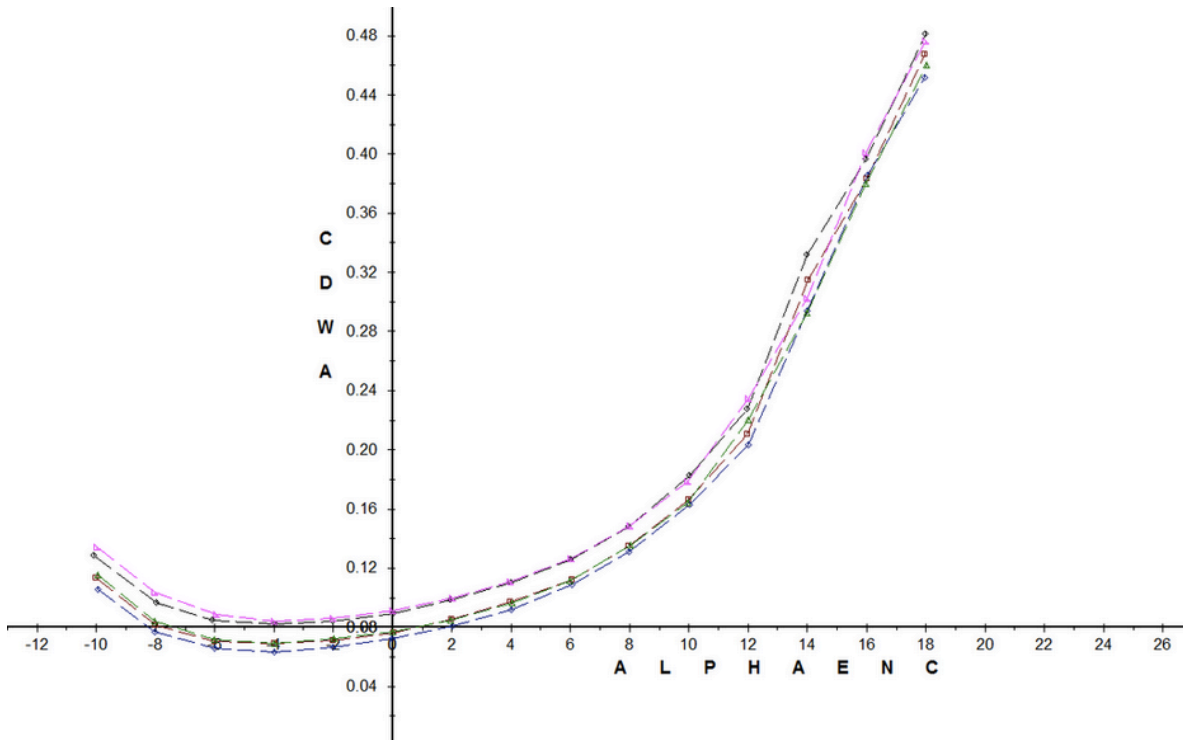


Fig. 4.8. Coefficient of drag vs. angle of attack at  $q = 1$  psf.

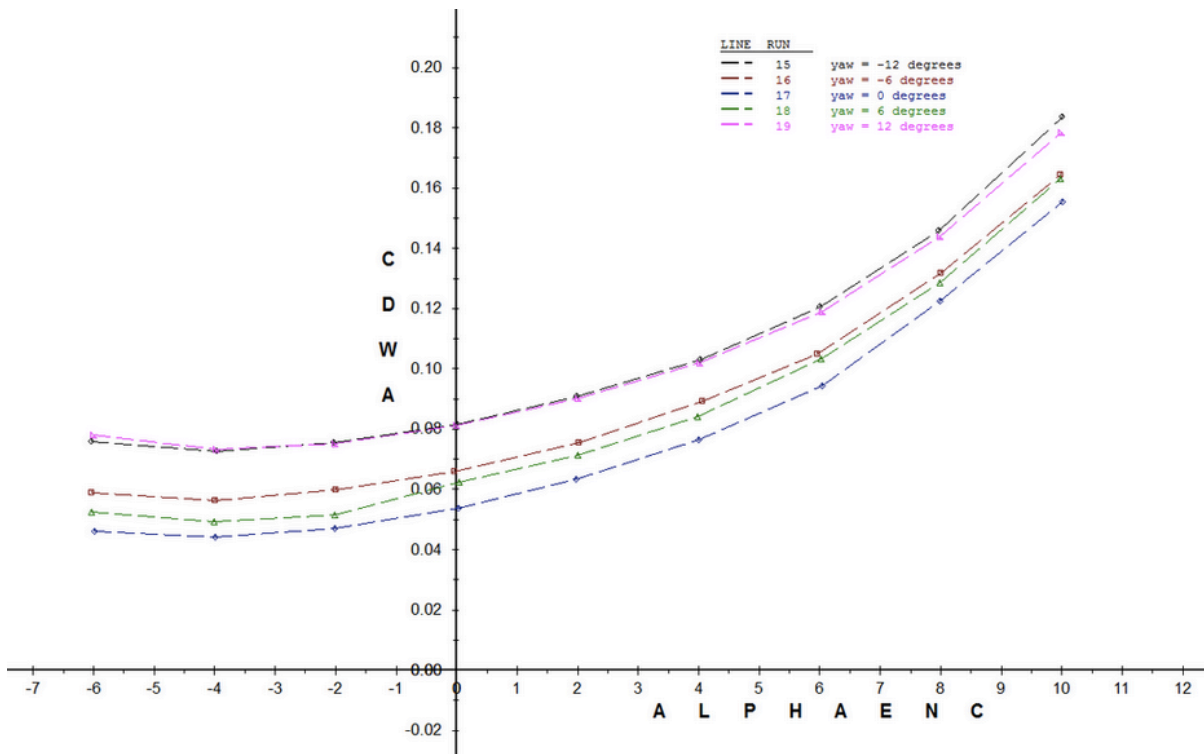


Fig. 4.9. Coefficient of drag vs. angle of attack at  $q = 6$  psf.



The drag polar for each dynamic pressure is shown in Fig. 4.10 and 4.11.

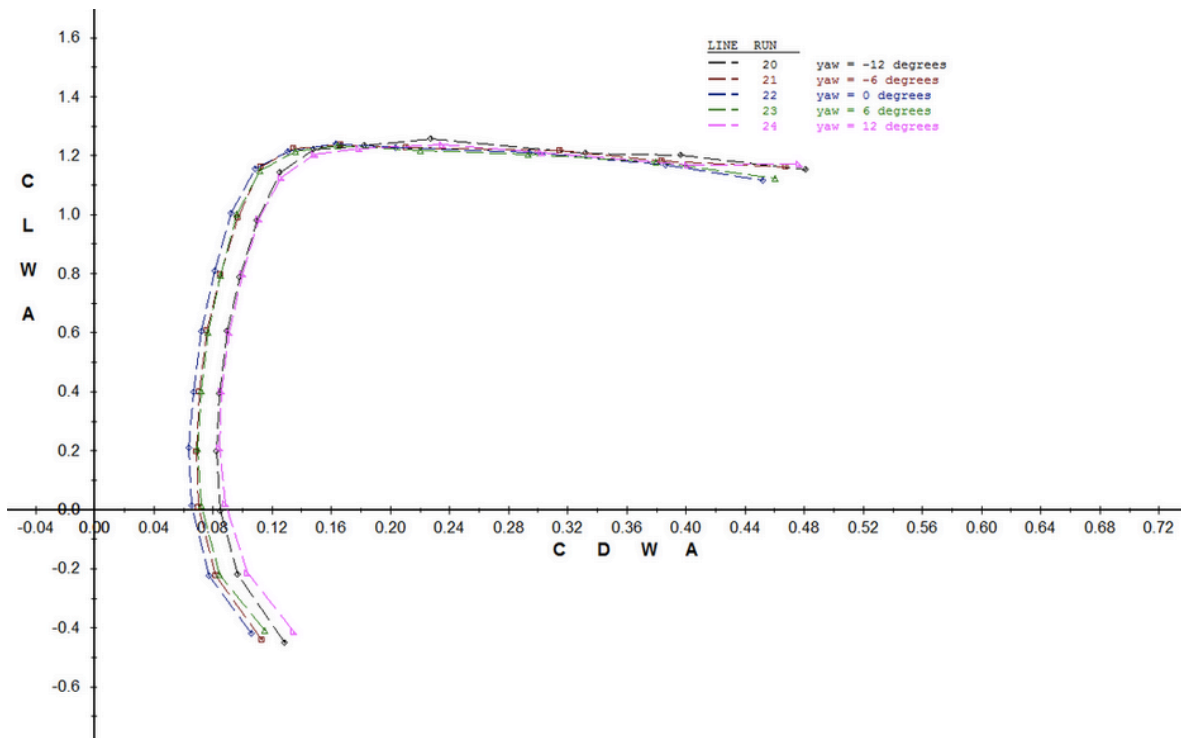


Fig. 4.10. Coefficient of lift vs. coefficient of drag at  $q = 1$  psf.

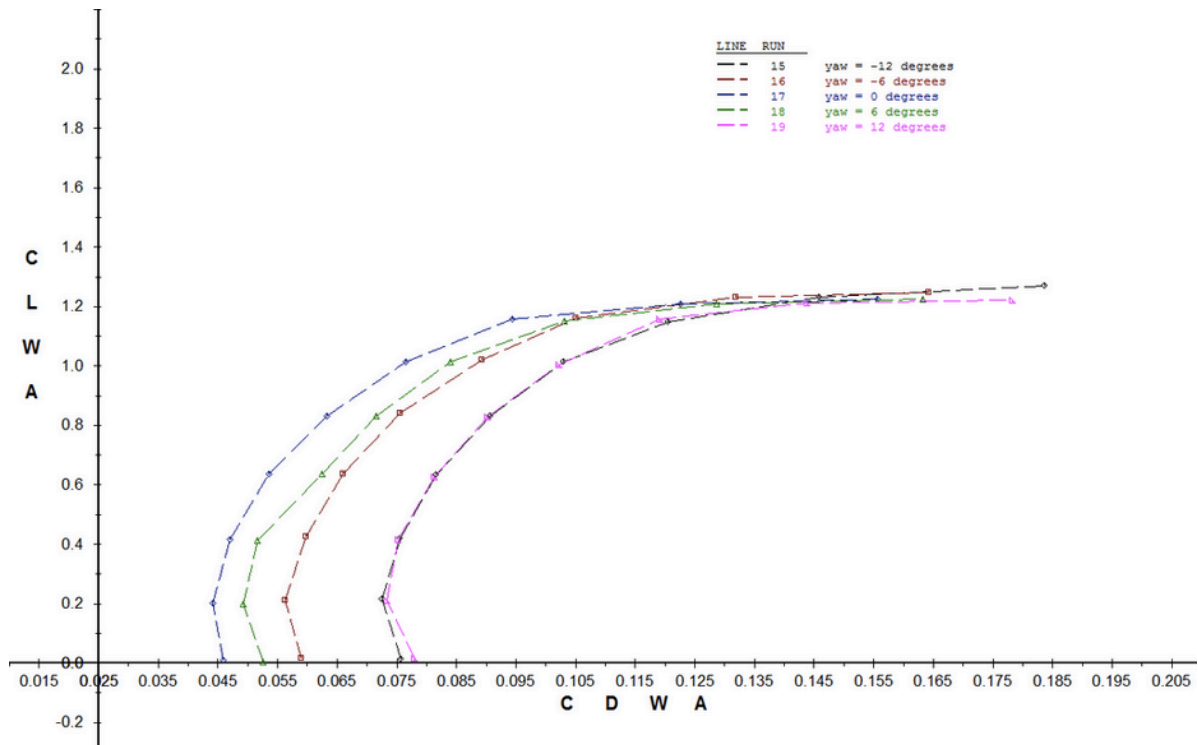


Fig. 4.11. Coefficient of lift vs. coefficient of drag at  $q = 6$  psf.



The coefficient of moment vs. angle of attack for each dynamic pressure is shown in Fig. 4.12 and 4.13.

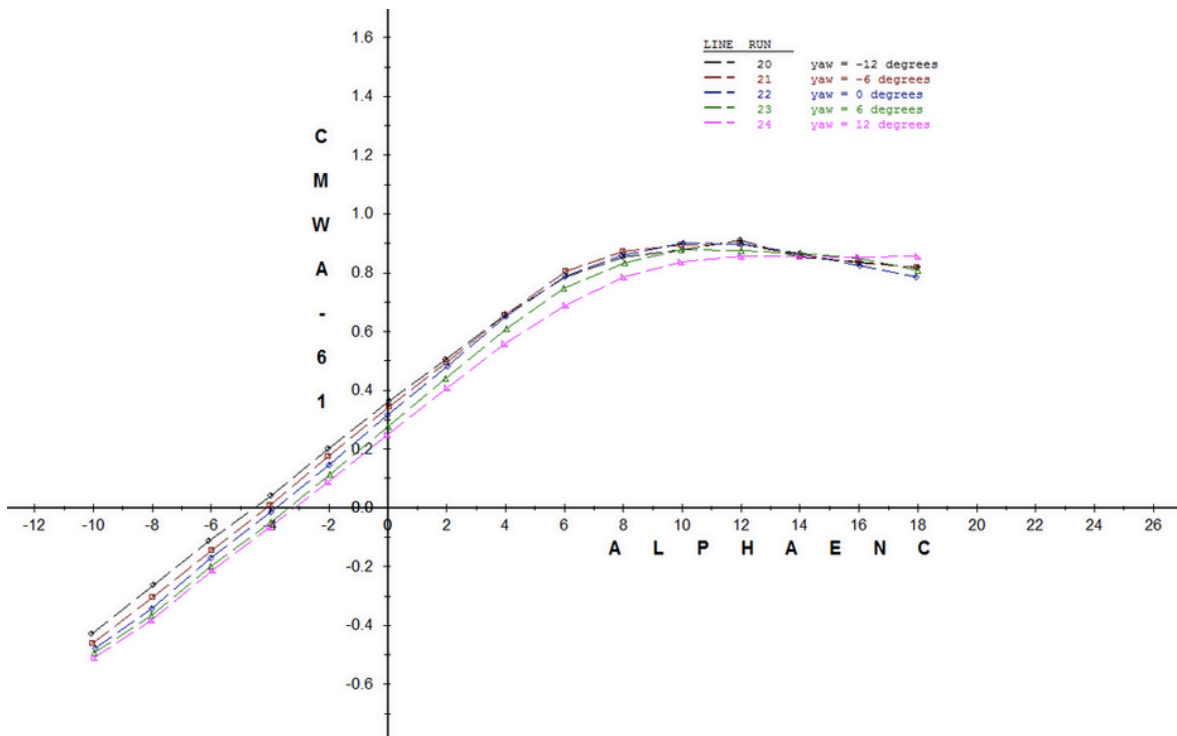


Fig. 4.12. Coefficient of moment vs. angle of attack at  $q = 1$  psf.

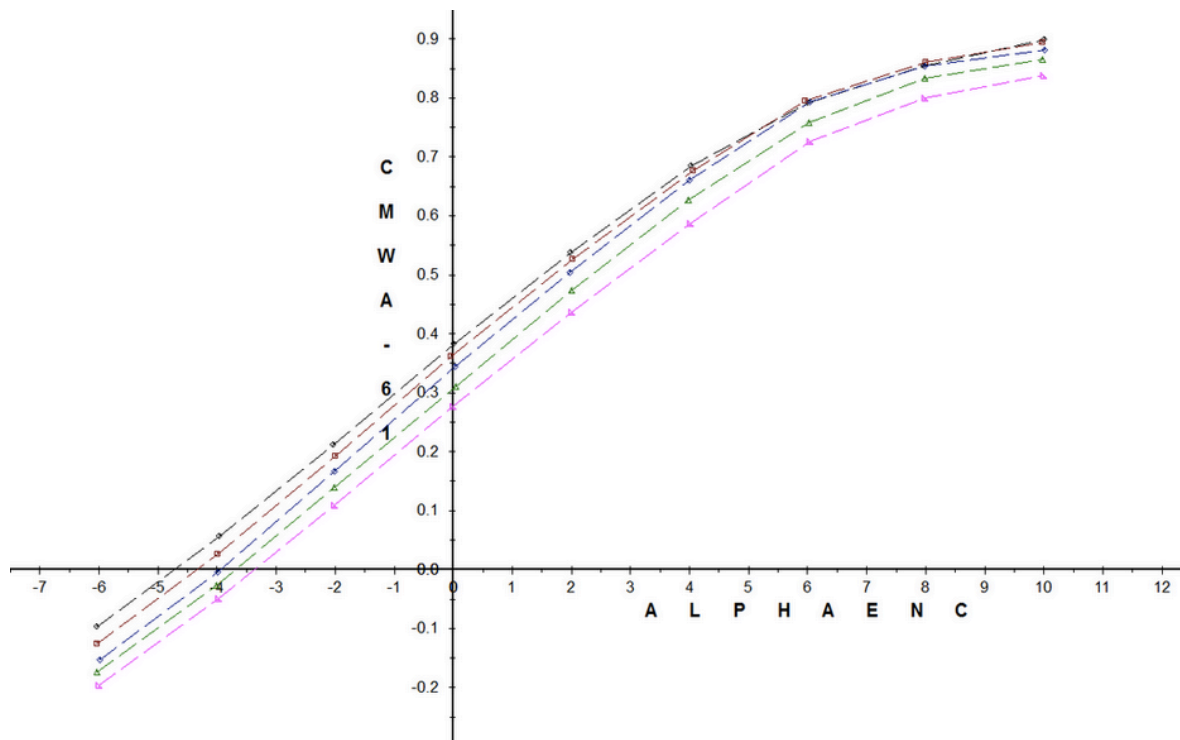


Fig. 4.13. Coefficient of moment vs. angle of attack at  $q = 6$  psf.



The pitching moment slopes above are characteristic of the model without tail surfaces. This means that the performance of the wing could be studied as a singular entity, and the tail could be designed to provide exactly the effect needed to ensure stability. A vital piece of information gleaned from the wind tunnel test was the lift center of the aircraft. Five virtual moment centers were chosen along the body of the craft, near the wing root. Force and moment data was computed for each of these points. Of particular interest in determining longitudinal stability characteristics is the change in pitching moment with respect to the angle of attack. By computing this slope at each of the five moment centers and interpolating between the points, the location where the slope was equal to zero was determined. This point corresponded to the aerodynamic force center of the wing.

## 4.4 Mission Model

### 4.4.1. Ground Taxi Mission

The requirements of the ground taxi mission are:

- Taxi across 40' x 8' of corrugated roofing panel.
- Navigate around three obstacles.
- Complete the mission within five minutes from the start.

Based on the power available tests, the aircraft will easily be able to produce enough thrust to navigate across the roofing panel, and complete the mission within five minutes.

### 4.4.2. Flight Mission 1

The requirements of Flight Mission 1 are:

- Lift off within the prescribed area.
- Complete as many laps as possible within the time limit.
- Land successfully.

Based on the lift generated in the wind tunnel test, the unloaded craft will easily be able to lift off within the 40 ft prescribed field length. The power available as well as the wing shape should allow for very quick flight through the course.

### 4.4.3. Flight Mission 2



The requirements for Flight Mission 2 are:

- Carry as many cargo blocks as possible.
- Lift off within the prescribed field length.
- Fly three laps.
- Land successfully.

The carrying capacity of 3 cargo blocks is a good compromise between cargo capacity and aircraft size. As discussed earlier, the size of the aircraft must change to accommodate more cargo blocks, which reduces overall flight score. The chosen cargo size represents a large amount of cargo, rendering the high lift airfoil necessary to lift off within the prescribed field length.

#### *4.4.4 Flight Mission 3*

The requirements for Flight Mission 3 are:

- Load 2 lb of payload simulating patients and attendants.
- Lift off within the prescribed area.
- Fly 3 laps within the shortest possible time.
- Land successfully.

Based on lift and power available as discovered throughout wind tunnel testing, the aircraft will be able to take off and perform this mission quickly.

## **5. DETAIL DESIGN**

We began our detailed design process with several main goals in mind; fast and simple manufacturing, durability and low weight. In order to achieve our goal of a fast manufacturing process we opted to try vacuum forming our fuselage shell from plastic. This required the design and construction of a thermo vacuum former. Using the thermo vacuum forming process allows fast reproduction of fuselage shells which can be varying in thickness and plastic type, and also allows many experimental internal structures to be tested. As progress was made on the thermo vacuum former, major road blocks prevented us from completing and testing the machine in a timely manner. Because we had initially decided to test both carbon fiber and vacuum formed plastic fuselages, the failure of the thermo vacuum former meant that we would build a carbon fiber fuselage.



## 5.1 Dimensional Parameters

Tables 5.1 – 5.3 contain the dimensions of the fuselage, wing, and tail while Table 5.4 contains the parameters of the propulsion system.

**Table 5.1** General Dimensions and Capacity

Fuselage dimensions	
Length	52.25 in
Height	7 in
Width	7 in

**Table 5.2** Detailed Wing Dimensions

Main wing	
Airfoil	FX 61-147
Span	74 in
Chord	8.89 in (constant)
Wing Area	553 in <sup>2</sup>
Aspect Ratio	7

**Table 5.3** Detailed Tail Dimensions

Tail	
Airfoil	flat
Horizontal Area	112 in <sup>2</sup>
Vertical Area	47 in <sup>2</sup>
Horizontal Span	24 in
Vertical Span	12.97 in

**Table 5.4** Detailed Propulsion Parameters

Propulsion	
Motor	2 x NTM 28-26a 1200KV
Gear ratio	Direct Drive
Batteries	Elite 1500 (2 x 11 cell pack)
Propellers	9x5

## 5.2 Structural Characteristics and Design

Our scoring analysis shows that the aircraft characteristics which have the largest impact on the total score are a high cruising speed and a low weight. Because the speed of the aircraft is directly connected to the weight, we made a light airframe our priority. All materials chosen are of high strength to density ratio. Composite materials such as carbon fibers, epoxy resin, fiberglass, and Kevlar fabrics were all thoroughly investigated. The final aircraft took advantage of properties of multiple materials such as lightweight foam, plywood sheeting, 3D printed ABS plastic and molded fiberglass and carbon fiber.

### 5.2.1 Main Wing

The structure of the main wing was designed to be light and fast to build. In order to meet these standards we chose to build the wings from a wire-cut foam core covered in plastic covering film. The foam cores were quick and easy to produce and offered good flexibility and durability, while the plastic film created a nice smooth finish.



### *5.2.2 Motor Mounts*

Because of the complexity of the motor mount, both in its shape and features, we opted to use a 3D printing process. This produced accurate and intricate parts that enabled us to optimize our design both aerodynamically and structurally, while keeping the design and construction process as simple as possible. Contained in the motor mounts, which are located on the main wings, are the motor, speed controller and fuse. The joint between the motor mount and the main wing spar created a structure strong enough in which to mount the landing gear. Integrating the landing gear mount into the motor mount proved to be an optimal use of our 3D printing capabilities, as it simplified the design further and reduced hand labor.

### *5.2.3 Fuselage*

The fuselage consists of an internal structure composed of laser cut plywood, 3D printed abs plastic, and carbon fiber. The outer shell was fabricated from carbon fiber and serves both aerodynamic and structural purposes. The method chosen to fabricate the carbon fiber shell was to mill a male mold from insulation foam and apply layers of carbon fiber and resin to make a one piece shell. When the resin was set, we poured acetone through a small opening in the carbon which broke down the foam and left only the carbon shell. Because we did not use a female mold, more work was required to achieve a smooth outer finish.

### *5.2.4 Tail*

The tail surfaces were cut from 10mm thick depron foam, and then coated in a plastic film like the main wing. This proved to be a simple and easy way to fabricate the tail surfaces and left ample room for modifications in size and shape.

### *5.2.5 Landing Gear*

The design of our landing gear was intended to maximize the aircraft's ability to navigate over the corrugated roofing panel while at the same time minimize the aerodynamic profile. These parameters required a more complicated approach than a large wheel, as a large wheel has a significant aerodynamic profile. Because the landing gear was somewhat complex in design and difficult to manufacture by hand we chose to 3D print several of the main parts. Below is an image of the landing gear design in the CAD software which shows the main features; A two-wheel base which pivots on a part connected to carbon fiber spars.

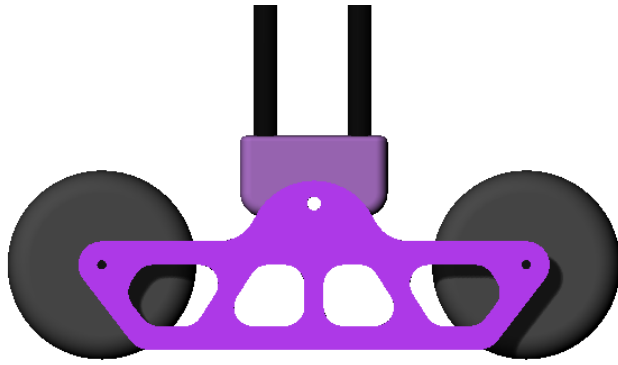


**Fig. 5.1.** The 3-D printed landing gear consists of a two-wheel base which pivots on a part connected to carbon fiber spars.

## 5.3 Systems and Sub-Systems Design, Component Selection, Integration and Architecture

### 5.3.1 Receiver

As a composite material for the fuselage was not decided until late in the design process, the receiver that was chosen was the Spektrum™ AR6255 6-Channel DSMX Carbon Fuselage Receiver. The carbon compatible receiver is a must if a carbon fiber fuselage is to be used, as carbon fiber is a conducting material, and thus the Faraday's cage effect must be considered. The carbon fuselage receiver thwarts this effect, and was so chosen allowing the team to choose a carbon fiber fuselage if it was seen as fit. Additionally, this receiver is a lightweight and compact package while still maintaining full range capabilities. The DSMX technology allows the receiver to be operated in the 2.4GHz band in close proximity to other aircraft on the same band, selecting separate channels to operate automatically to avoid interference or "lock out". As this receiver is a 6-Channel receiver, it is fully capable of handling the required number of channels that the design requires.

### 5.3.2 Batteries

As the power output of the batteries is directly proportional to the voltage placed across the motors, it was decided to create 10 cell NiMH battery packs made with Elite 1500 mAh cells. Given that the servos and receiver only call for an operating voltage of 4.8V, a smaller four cell NiMH battery was chosen for the receiver pack.



### 5.3.3 Speed controller and motors

The motors chosen were of the brushless type, with a limited current of 18A. As such, a brushless speed controller rated at greater than 20A was sought. Two Turnigy 25-Amp Airplane Brushless ESC's were ultimately chosen. Despite the fact that the motor could potentially draw over 15A for brief periods of time, it was assumed that the 25A speed controller could withstand the higher current without burning out given the rated amperage level, as well as the fact that the circuit would be protected with a 15A fuse. Table 5.5 gives a summary of the control system components while Table 5.6 gives the specifications of the control system components. Figure 5.2 shows the flow-chart of the systems circuit.

**Table 5.5** Control System Component Summary

Component Name	Component Description
HITEC HS-65	Aileron servo
HITEC HS-85	Tail servo
HITEC HS-65	Flap servo
Spektrum™ AR6255 6-Channel DSMX Carbon Fuselage Receiver	Receiver
4 Cell KAN 400 2/3AAA NiMH	Receiver Battery Pack
Turnigy 25 amp Brushless ESC	Speed Controller

**Table 5.6** Control System Component Specifications

Servo	Weight [oz]	Torque @ 4.8V [oz-in]	Speed @ 4.8V [s/60°]
HITEC HS-65	0.39	25	0.14
HITEC HS-85	0.3	15	0.17

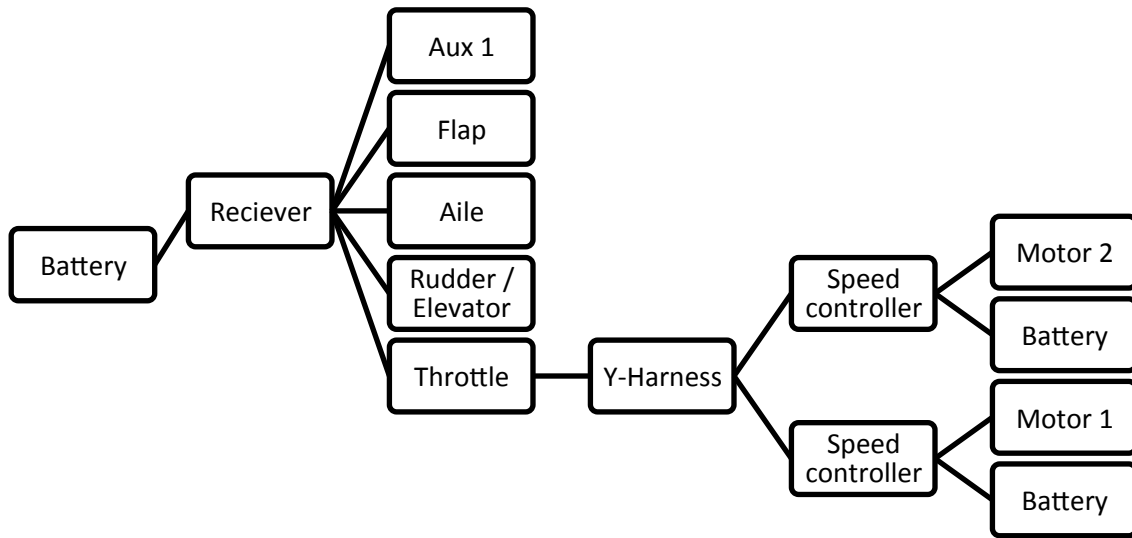


**Fig. 5.2** Systems Circuit Flow-Chart

## 5.4 Weight and Balance

The weight and balance tables were based on component weights and distance from the leading edge of the wing, which served as a datum. The battery location was adjusted to keep the CG consistent in each mission. For the following tables, the x-axis corresponds to the longitudinal axis, y-axis corresponds to the lateral axis, and z-axis corresponds to the yaw axis. Tables 5.7-5.9 contain the weight and balance for each flight mission.

**Table 5.7** Weight and balance of the empty aircraft.

Empty	Weight (lb)	CG location (in)	
		x	y
Airframe	2.20	0	18.92-33.33
Motor	.352	9 and -9	5
Propeller	0.011	9 and -9	6
Tail Servos	0.084	1 and -1	-25
Aileron Servos	0.049	17.25 and -17.25	3
Radio receiver	0.011	0	-20



**Table 5.8.** Weight and balance of the aircraft with 6" Cubes.

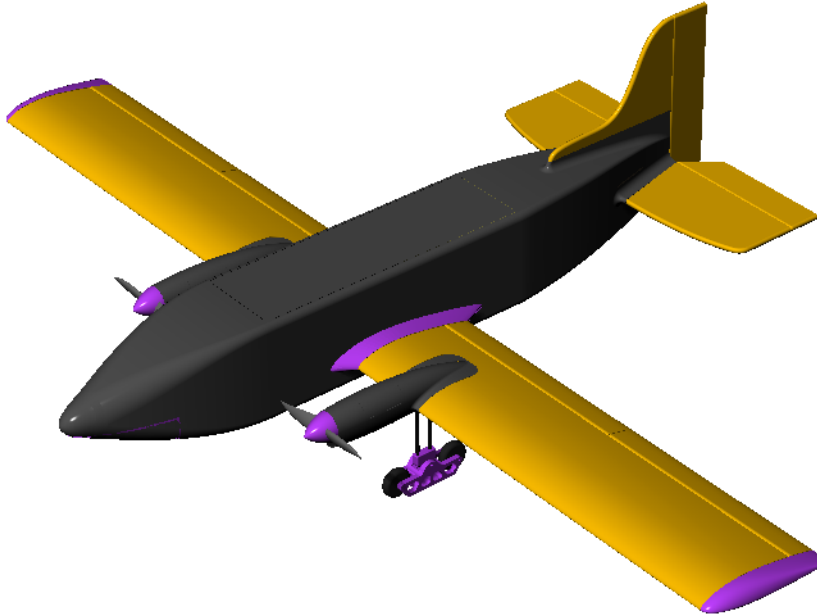
Mission 1	Weight (lb)	CG Location (in)	
		x	y
Aircraft Empty	2.71	0	18.92-33.3
Block 1	1.0	0	4
Block 2	1.0	0	-3
Block 3	1.0	0	-9

**Table 5.9.** Weight and balance of the aircraft for emergency medical mission.

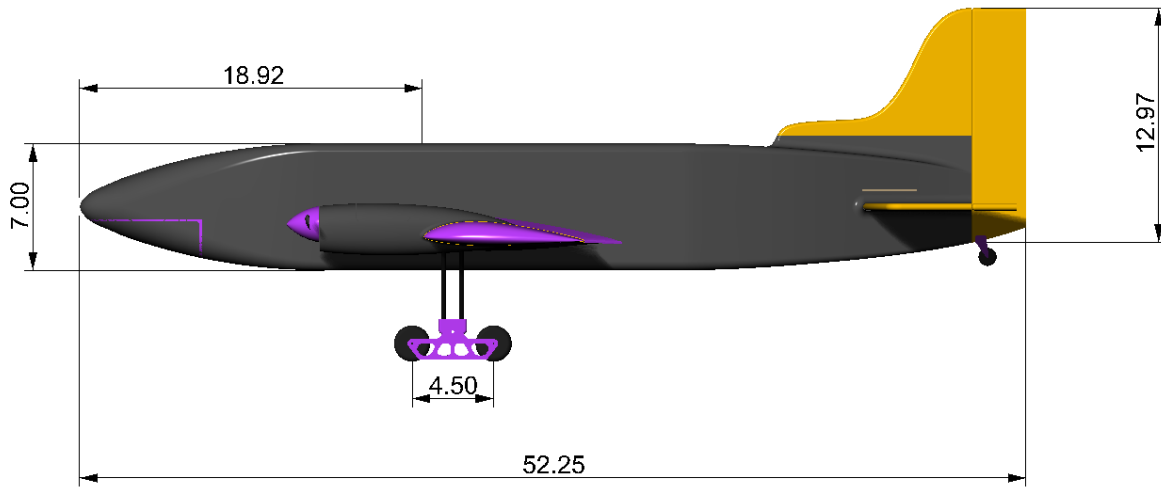
Mission 2	Weight (lb)	CG Location (in)	
		x	y
Aircraft Empty	2.71	0	19.29
Block 1	1.0	0	14.5
Block 2	1.0	0	7.07

## 5.5 Drawing Package

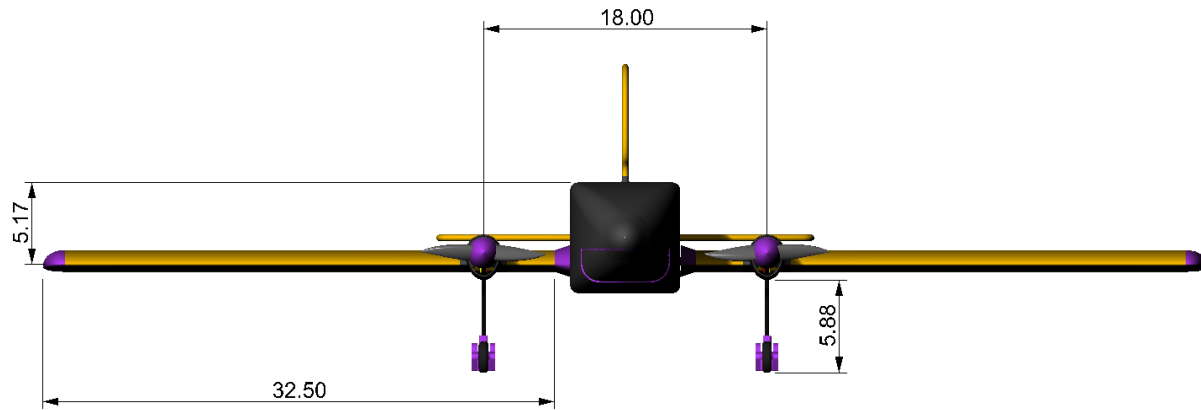
All units for the drawing package are in inches.



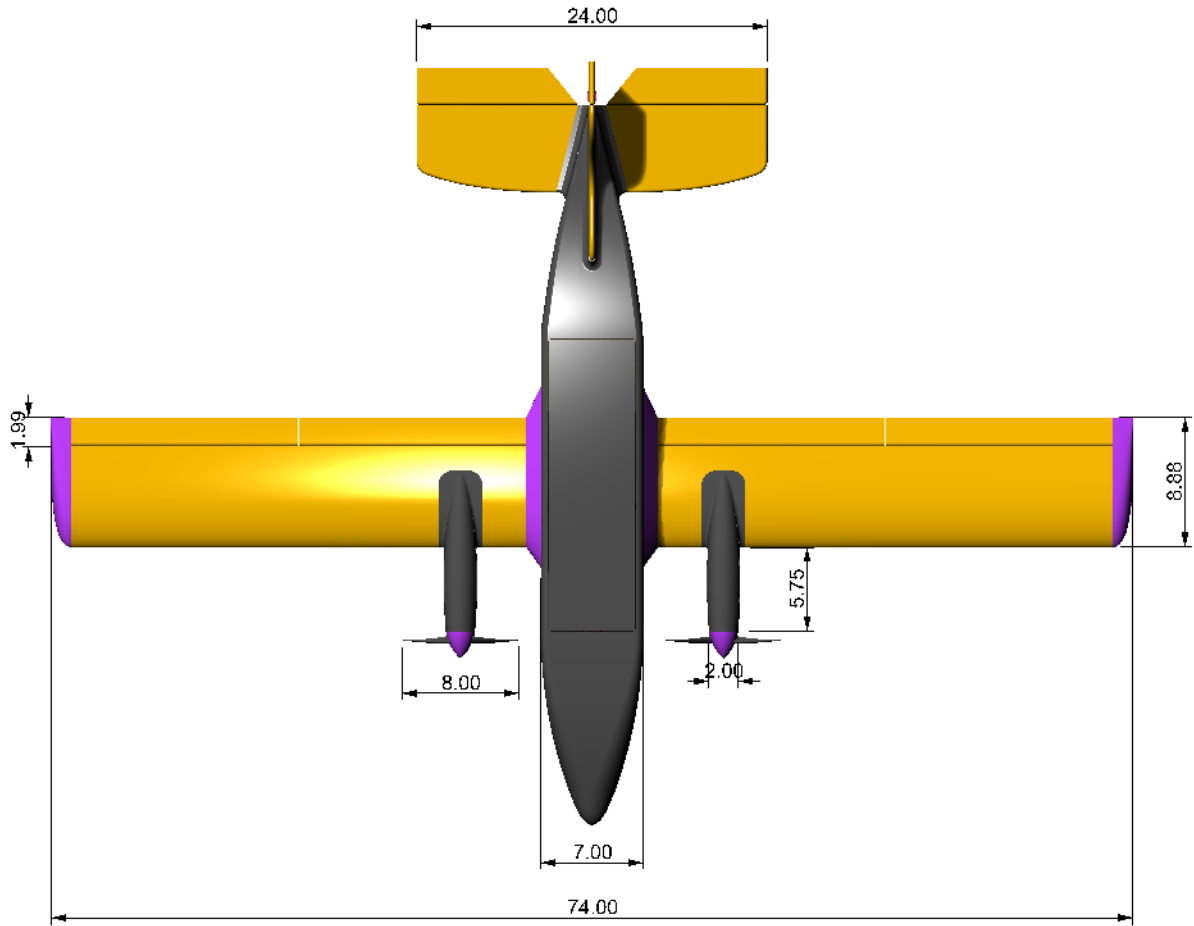
**Perspective View**



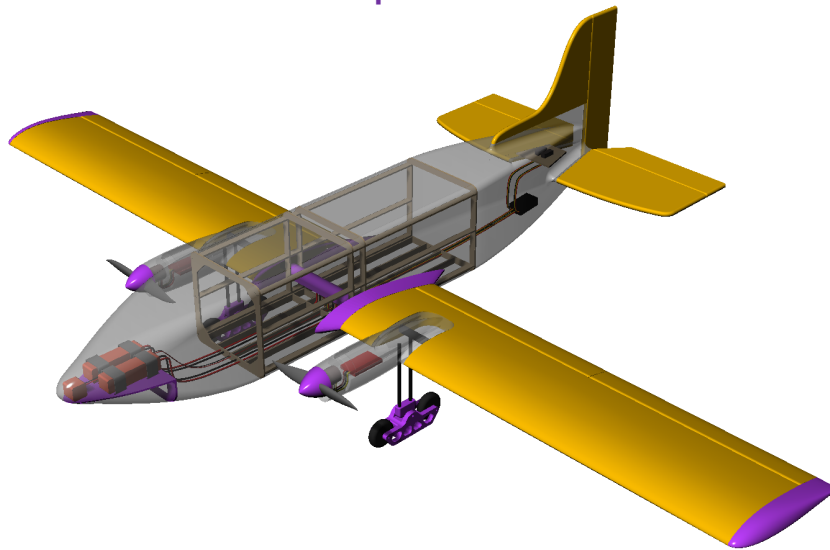
Side View



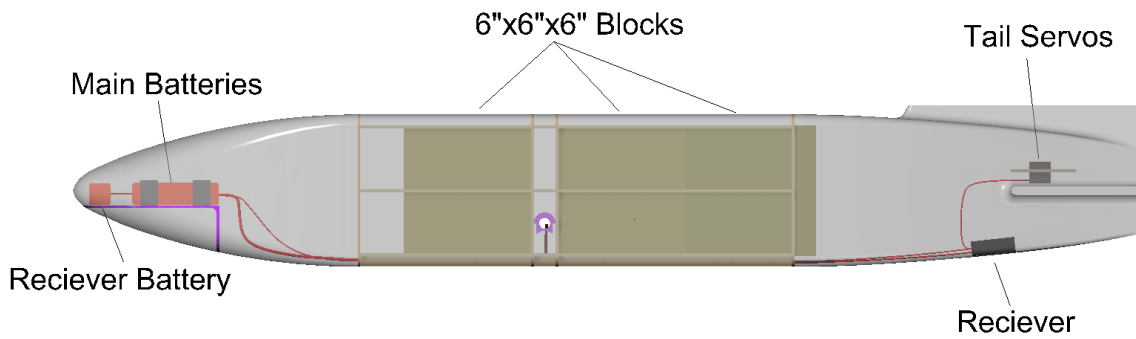
Front View



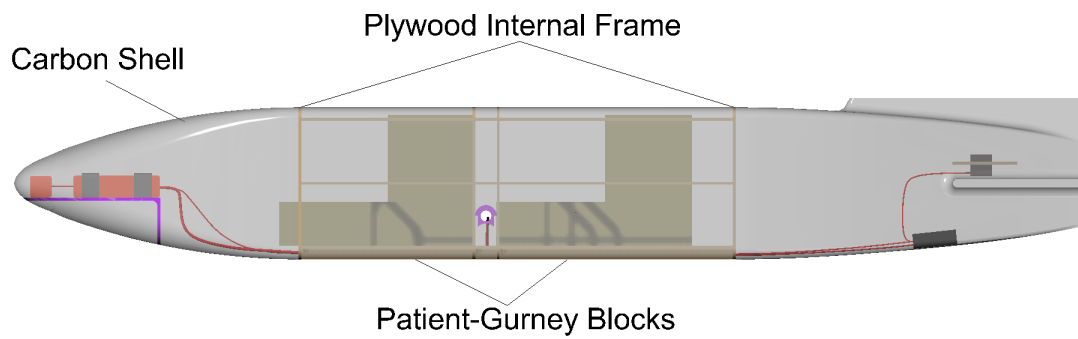
Top View



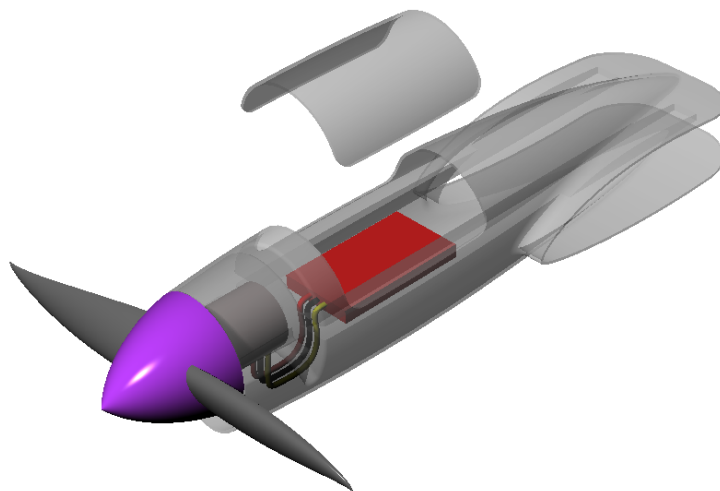
Transparent Perspective View



**Internal Layout and 6" cube payload.**



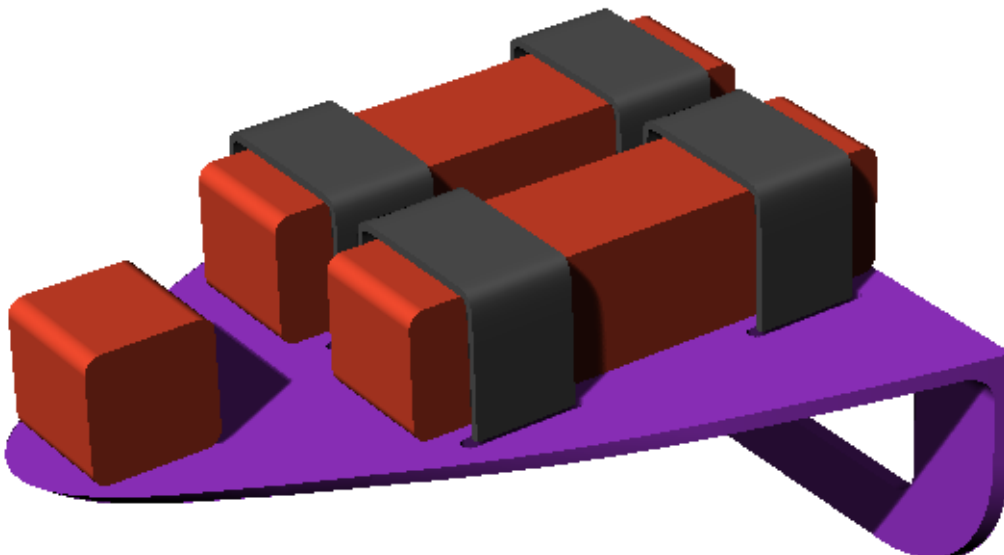
**Patient-Gurney Payload**



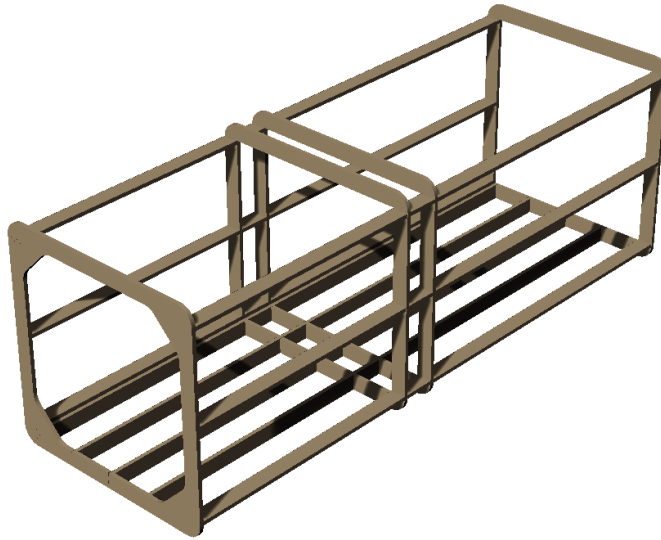
**3D printed motor mount**



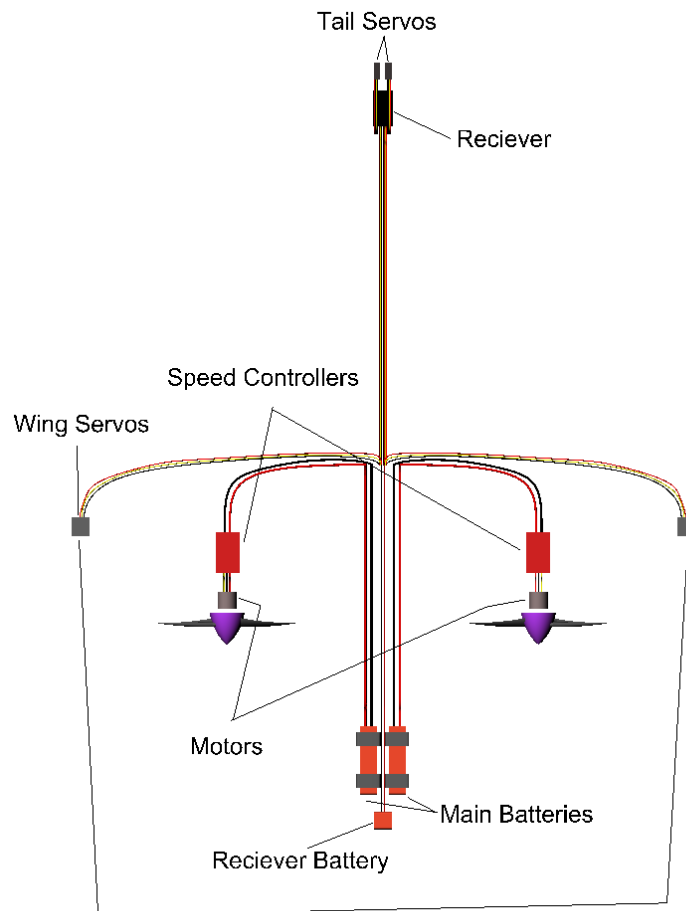
3D printed landing gear



3D printed battery mount with batteries and Velcro shown



**Internal plywood structure/payload mounting**



**Wiring and electronics schematic**



## 6. MANUFACTURING PLAN AND PROCESSES

The fabrication of the Dawg Sled is a culmination of incorporating flight and aerodynamics knowledge in design, tests in the University of Washington Kirsten wind tunnel for aerodynamic performance data, manufacturing test models as well as individual construction of the fuselage, wing, the empennage, and a unique landing gear to accommodate competition scenarios. During the testing phase of our model, any member of the plane that would be facing aerodynamic affects were tuned up for maximized performance through hand analysis and calculation with some assistance with software computation.

### 6.1 Production Plan and Schedule

After the preliminary design of our aircraft was completed, a schedule was created in order to efficiently and rapidly construct our test model and competition model. A timeline of our schedule is shown below in Fig. 6.1:

Task	December					January				February				March				
	1-	8-	15-	22-	29-	5-	12-	19-	26-	2-	9-	16-	23-	1-	8-	15-	22-	29-
Wind Tunnel Model	█	█	█															
Wings	█																	
Carbon Fiber	█																	
Fuselage		█																
Tail			█															
Servos and Wiring			█															
Flight Test Model						█	█	█	█									
Center Wing Section						█				█								
Outer Wing Sections							█				█							
Carbon Fiber								█				█						

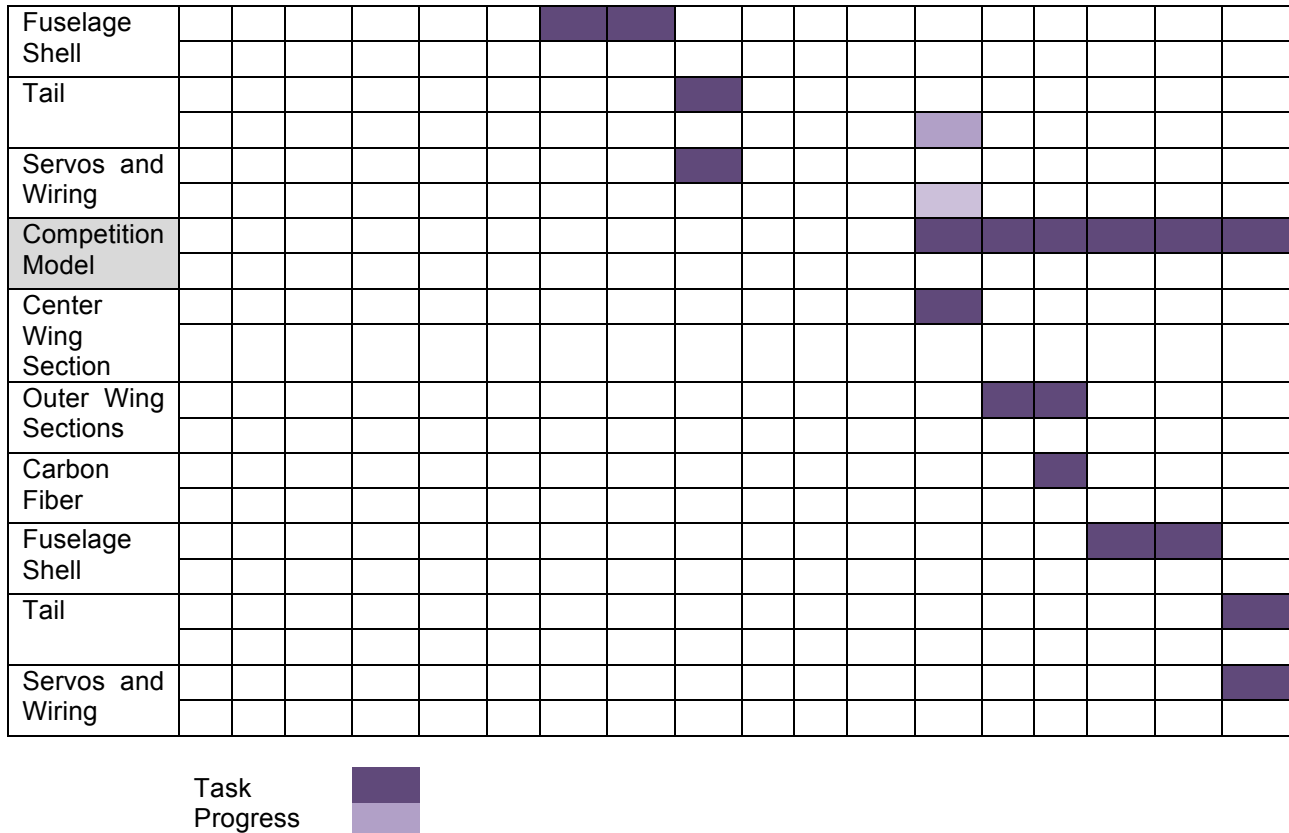


**Fig. 6.1.** Manufacturing Timeline

## 6.2 Manufacturing Process

The manufacturing process was broken up into three distinct areas: fuselage, wings, and empennage.

### 6.2.1. Fuselage

During the building phase of our prototype model, our fuselage was constructed out of foam with aluminum covering. Depron foam was used due to the expeditious nature and ease of manipulation that resulted in the availability to test as soon as possible. The metal tape skin was used to eliminate the adverse effects that the foam would induce on aerodynamic data and mimic the characteristics of the skin on our final model to maintain consistency of aerodynamic effects. The foam was cut and formed using a band saw and sanding, wrapped in metal tape and then mounted on a testing strut. The test data received from wind tunnel testing at the University of Washington Kirsten Wind Tunnel provided valuable data that was used to confirm aerodynamic stability as well as provide model in which we could improve on.



Our final fuselage model comprised of a filleted rectangular carbon fiber shell resembling a stretched airfoil shape with an internal framework composed of plywood. Manufacturing of the shell entailed the creation of a mock up model in Solidworks for quick analysis and the laying of carbon fiber in a 45-degree layering technique on a foam mold for the physical creation of the fuselage. The carbon fiber shell which is essentially the skin of the fuselage was constructed with the intent of the ability to manage torsional loads as well as maintain rigidity in addition to the internal structure such that the aerodynamic shape is maintained.

The individual internal structure components were shaped using laser cutting and assembly of plywood. The plywood spars and rib structure maintained our design intent of a good strength to weight ratio material as well as the ability to securely attach the passengers for the payload mission such that the flight characteristics of the airplane would change a minimal amount and maintain an aerodynamic center above the wings. Compartments were constructed in the internal structure to house electronics in the nose area and cargo above the wings.

### *6.2.2. Wings*

The test model of our wing was built in a similar fashion to the fuselage; depron foam with metal tape skin. A tube-like copper spar was added at the most thick part of the wing for added structural support and acted as an attachment point to the fuselage. Rapid manufacturing of multiple wing test models allowed from refinement in our design and improved flight efficiency of our final wing.

The FX61-147 airfoil wings that were produced consisted of wire cut foam. The FX61-147 airfoil shape was chosen due to the known reliability and flight characteristics to provide lift from previous flight experiments. The use of foam for the wings is due to the lightweight characteristics as well as structural traits that would resist adverse mechanical effects. Also, the foam structure has a good strength to weight ratio that is utilized to maintain aerodynamic affects efficiency to provide performance lift at required levels without failing or deforming. A carbon spar was added in each wing to provide an extra factor of strength in the wings to aid in resisting deformation. The minimalist nature of a one piece wing of foam with a carbon spar provided maximal axial, torsional, and transverse force support while having a lowered manufacturing time.

### *6.2.3. Empennage*

Construction of the conventional tail components was similar to the main wings. Depron foam cored tails were wire cut and wrapped in plastic film in the same fashion as the main lift wings for the ease and expeditious nature on manufacturing.



### 6.2.4 Landing Gear

The ski-landing gear was developed to accommodate the first mission of the competition. The skis were to assist in navigating the corrugated panels with ease by providing a stable platform in which the wheels would not become stuck. The skis were designed in Solidworks, printed and constructed of the same plastic, which provided a high strength to weight ratio.

### 6.2.5 Motor and Battery Mounts

Three-dimensional printing was utilized to manufacture the motor and battery mounts for use in our final model. The motor mount was designed using 3-D modeling software to encompass lightweight characteristics and aerodynamic efficiency while being able to adequately house our vehicular mobility units. The battery mount was modeled such that the housing would fit in the nose area of our fuselage. This simple design and feature allowed us store our batteries in an expendable location while also improve our flight characteristics by moving the center of gravity forward.

## 7. TESTING PLAN

Tests were conducted to determine the performance of all components on the prototype aircraft. The purpose of the tests was to compare the actual performance versus the performance predicted by the design team. These included aerodynamic, propulsion, structure, flight, and ground testing. The results offered validation for predicted designs and determined the functionality of essential components. Figure 7.1 provides a checklist of each component tested and the objective of each test.

<b>Aerodynamic Testing</b>	
• Determine optimal placement of tail and wing.	<input checked="" type="checkbox"/>
• Determine flight characteristics for optimal flight.	<input checked="" type="checkbox"/>
<b>Propulsion Testing</b>	
• Determine optimal motor and propeller combination.	<input checked="" type="checkbox"/>
<b>Structure Testing</b>	



<ul style="list-style-type: none"> <li>• Ensure wing reliability to support a full load in 2 g turns.</li> </ul>	☑
<ul style="list-style-type: none"> <li>• Ensure landing gear reliability to withstand 3 g shock with full load.</li> </ul>	☑
<b>Flight Testing</b>	
<ul style="list-style-type: none"> <li>• Limit takeoff distance to within 40 ft by 40 ft box.</li> </ul>	☑
<ul style="list-style-type: none"> <li>• Allow pilot to familiarize with aircraft handling and mission course.</li> </ul>	☑
<ul style="list-style-type: none"> <li>• Measure performance of all missions.</li> </ul>	☑
<b>Ground Testing</b>	
<ul style="list-style-type: none"> <li>• Ensure aircraft can reliably maneuver over corrugated roofing.</li> </ul>	☑

**Fig. 7.1.** Checklist of objectives to be completed by testing

A schedule of tests performed is shown in Figure 7.2.

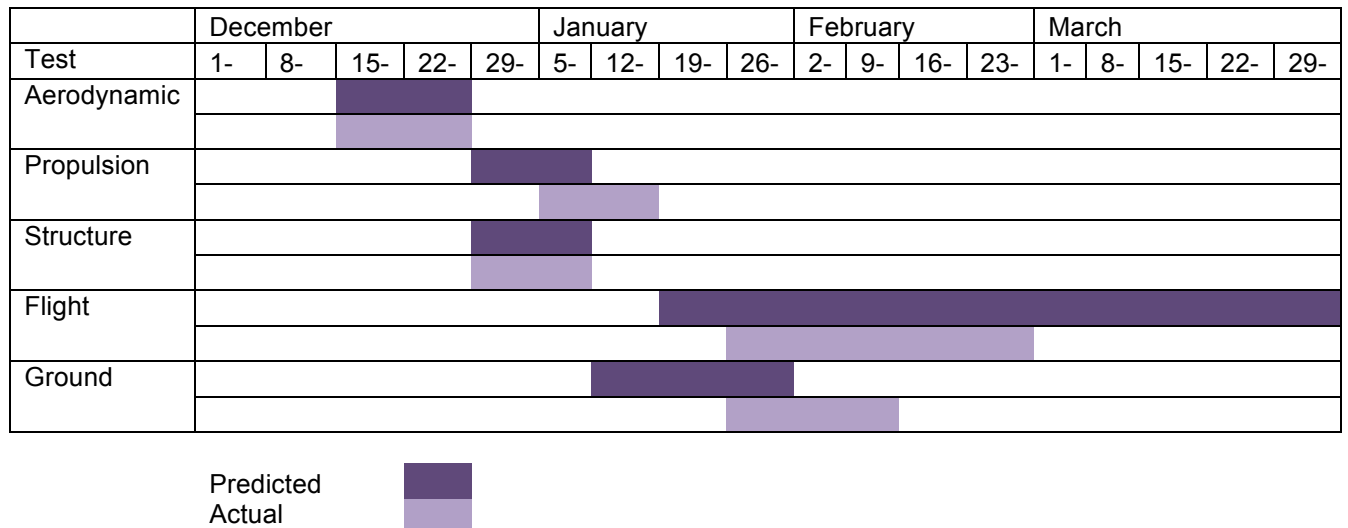


**Fig. 7.2.** Schedule of predicted and actual testing times

### 7.1.1 Aerodynamic testing



Aerodynamic testing was conducted in the Kirsten Wind Tunnel, at the University of Washington. The results of wind tunnel tests gave an accurate representation of how the aircraft would perform in actual flight and effectively solidified the design of the aircraft.

Tail-off testing was performed in order to allow for the tail to be designed specifically to offset the pitching moments seen by the wing-body combination. This was a more effective testing method than placing an arbitrary tail on the plane. A full authority balance allowed for the prototype model to be pitched and yawed to any combination of angle desired during testing. Variation of dynamic pressure, angle of attack, yaw angle, and control surface settings resulted in measurements of roll and tail moments, lift, and drag. These measurements were necessary to be able to calculate the lift, drag and moment coefficients of the aircraft. The physical data from the wind tunnel testing allowed for improvement in efficiency of sizing issues and placement for the tail and main wing, determination of the aerodynamic center of the wing-body combination, and locate the necessary center of gravity location.

#### *7.1.2 Propulsion Testing*

Propulsion testing was conducted in the 3ft by 3ft Wind Tunnel at the University of Washington. This dynamic testing was determined to be a more accurate representation of the performance of the motor and propeller combination than static testing given flight conditions and the competition location which is prone to high wind conditions. The motor/propeller combinations were tested at a dynamic pressure of 1 psf and 6 psf to simulate take-off and in-flight conditions. The most effective combination was determined to have the highest performance in flight but still have enough thrust for the restricted take-off.

#### *7.1.3 Structure Testing*

Structure testing was performed on the wing-body and the landing gear as the limiting structural components. A wingtip test was conducted to test the wing-body and struts. This was simulated to be able to withstand double the expected maximum load. The landing gear was also tested statically to withstand double the expected load but at a predicted 3 g to account for impact.

#### *7.1.4 Flight Testing*

Flight-testing was performed with the first prototype to determine overall performance of the aircraft. The pilot was able to become familiar with the aircraft handling and the mission routes as well as determine the stability characteristics of the aircraft. Extensive flight testing was allowed for future prototypes to guarantee familiarity in order to account for unpredictable circumstances in weather at the competition site.



### *7.1.5 Ground Testing*

Ground testing was performed to determine the functionality of the landing gears. The full prototype aircraft was tested for maneuverability over corrugated roofing panel. The aircraft was tested to make left and right turns as well as travel diagonally across the panels. Multiple runs were conducted to ensure reliability, given the importance of the ground mission.

## **8. PERFORMANCE RESULTS**

During initial flight-testing we encountered several issues regarding the location of the center of gravity of our aircraft. On the first takeoff attempt the aircraft left the ground and it became immediately apparent that the stability of the aircraft was impaired due to a tail heavy center of gravity. The aircraft was safely landed and the batteries moved farther forward to offset the tail-heavy effect. On the second flight attempt the stability of the aircraft was greatly improved, and it was decided to conduct maneuverability testing. The over all flight performance was close to our goal, however the control sensitivity was not calibrated to an ideal state. The elevator was too sensitive, making landing and altitude consistency difficult, while the ailerons were not sensitive enough, impairing the aircrafts ability to perform quick turns. Appropriate measures were taken to properly calibrate the control surface deflection. After we were confident in the aircrafts controllability and stability we attempted to carry the payload configurations. Our first attempt was with the three 6" cubes, and not only did the aircraft take off well within the 40ft limit, it maintained its stability and controllability as well. The patient-gurney test flight had the same results as the blocks. After the initial flight tests we conducted taxi tests on corrugated roofing panels. We replicated the taxi mission's layout and attempted to complete the requirements. The landing gear did its job well in this test and we felt confident in the aircraft's ability to navigate over the roofing panels and around the obstacles. Because our aircraft performed well in the desired areas, we concluded that no major changes should be made to the shape or size of the aircraft. However we felt that we could still focus on improving the construction technique to decrease weight and increase durability.



## 9. REFERENCES

<sup>1</sup> AIAA, "2012/13 Rules and Vehicle Design", October 2012. Accessed 9/25/12.  
[[http://www.aiaadbf.org/2013\\_files/2013\\_rules.htm](http://www.aiaadbf.org/2013_files/2013_rules.htm)]

[1] Raymer, Daniel P. *Aircraft Design : A Conceptual Approach*. Reston, VA: American Institute of Aeronautics and Astronautics, 1999. Print.